The Journal of Immunology

Mycobacterial Cord Factor Reprograms the Macrophage Response to IFN- γ towards Enhanced Inflammation yet Impaired Antigen Presentation and Expression of GBP1

Alexandra Huber, Barbara Killy, Nadine Grummel, Barbara Bodendorfer, Sushmita Paul, Veit Wiesmann, Elisabeth Naschberger, Jana Zimmer, Stefan Wirtz, Ulrike Schleicher, Julio Vera, Arif Bülent Ekici, Alexander Dalpke and Roland Lang

J Immunol 2020; 205:1580-1592; Prepublished online 12 August 2020;
doi: 10.4049/jimmunol.2000337
http://www.jimmunol.org/content/205/6/1580

The Journal of Immunology is published twice each month by
The American Association of Immunologists, Inc.,
1451 Rockville Pike, Suite 650, Rockville, MD 20852

Print ISSN: 0022-1767 Online ISSN: 1550-6606.

Mycobacterial Cord Factor Reprograms the Macrophage Response to IFN-γ towards Enhanced Inflammation yet Impaired Antigen Presentation and Expression of GBP1

Alexandra Huber,* Barbara Killy,* Nadine Grummel,* Barbara Bodendorfer,* Sushmita Paul,† Veit Wiesmann,‡ Elisabeth Naschberger,§ Jana Zimmer,¶ Stefan Wirtz,‖ Ulrike Schleicher,* Julio Vera,† Arif Bülent Ekici,# Alexander Dalpke,¶, and Roland Lang***

Mycobacteria survive in macrophages despite triggering pattern recognition receptors and T cell–derived IFN-γ production. Mycobacterial cord factor trehalose-6,6-dimycolate (TDM) binds the C-type lectin receptor MINCLE and induces inflammatory gene expression. However, the impact of TDM on IFN-γ–induced macrophage activation is not known. In this study, we have investigated the cross-regulation of the mouse macrophage transcriptome by IFN-γ and by TDM or its synthetic analogue trehalose-6,6-dibehenate (TDB). As expected, IFN-γ induced genes involved in Ag presentation and antimicrobial defense. Transcriptional programs induced by TDM and TDB were highly similar but clearly distinct from the response to IFN-γ. The glycolipids enhanced expression of a subset of IFN-γ–induced genes associated with inflammation. In contrast, TDM/TDB exerted delayed inhibition of IFN-γ–induced genes, including pattern recognition receptors, MHC class II genes, and IFN-γ–induced GTPases, with antimicrobial function. TDM downregulated MHC class II cell surface expression and impaired T cell activation by peptide-pulsed macrophages. Inhibition of the IFN-γ–induced GTPase GBP1 occurred at the level of transcription by a partially MINCLE-dependent mechanism that may target IRF1 activity. Although activation of STAT1 was unaltered, deletion of Socs1 relieved inhibition of GBP1 expression by TDM. Nonnuclear Socs1 was sufficient for inhibition, suggesting a noncanonical, cytoplasmic mechanism. Taken together, unbiased analysis of transcriptional reprogramming revealed a significant degree of negative regulation of IFN-γ–induced Ag presentation and antimicrobial gene expression by the mycobacterial cord factor that may contribute to mycobacterial persistence. ***The Journal of Immunology*****, 2020, 205: 1580–1592.**

Mycobacterium tuberculosis is arguably the most successful bacterial pathogen, and it manages to survive and replicate intracellularly in the phagosome of macrophages. Blockade of phagosomal maturation and acidification is an essential mechanism of mycobacterial virulence, which is counteracted by activation of the macrophage by T cell–derived IFN-γ. However, *M. tuberculosis* interferes with the full execution of the macrophage response to IFN-γ, especially increased Ag presentation via MHC class II (MHC-II) (1–3). Thus, exposure to *M. tuberculosis* regularly results in the establishment of latent infection, a stalemate of the host–pathogen interaction, which may result in reactivation tuberculosis whenever cellular immunity wanes and intracellular mycobacteria are allowed to proliferate again.

The mycobacterial cell wall contains a plethora of glycolipids and is especially rich in trehalose-6,6'-dimycolate (TDM), also termed cord factor because it is thought to cause the high hydrophobicity of the cell wall and clumping (cording) of mycobacteria in culture in vitro. TDM appears to play an important role in the infection biology of tuberculosis because it can evoke, per se, crucial aspects of the host response [i.e., the formation of granulomas after i.v. injection (4, 5), stimulation of macrophages

*Institut für Klinische Mikrobiologie, Immunologie und Hygiene, Universitätsklinikum Erlangen, Friedrich-Alexander Universität Erlangen-Nürnberg, D-91054 Erlangen, Germany; †Laboratory of Systems Tumor Immunology, University Hospital Erlangen and Friedrich-Alexander University Erlangen-Nürnberg, D-91054 Erlangen, Germany; ‡Fraunhofer-Institut für Integrierte Schaltungen, D-91058 Erlangen, Germany; §Molekulare und Experimentelle Chirurgie, Universitätsklinikum Erlangen, Friedrich-Alexander Universität Erlangen-Nuremberg, D-91054 Erlangen, Germany; ¶Department of Infectious Diseases, University Hospital Heidelberg, D-69120 Heidelberg, Germany; ‖Medizinische Klinik 1, Universitätsklinikum Erlangen, Friedrich-Alexander Universität Erlangen-Nürnberg, D-91054 Erlangen, Germany; #Institut für Humangenetik, Universitätsklinikum Erlangen, Friedrich-Alexander Universität Erlangen-Nürnberg, D-91054 Erlangen, Germany; and **Institut für Medizinische Mikrobiologie und Hygiene, Technische Universität Dresden, 01307 Dresden, Germany

ORCIDs: 0000-0002-7526-6562 (A.H.); 0000-0002-2338-3919 (B.K.); 0000-0001-7327-9311 (V.W.); 0000-0001-6936-7431 (S.W.); 0000-0003-1648-6618 (A.D.); 0000-0003-0502-3677 (R.L.).

Received for publication March 26, 2020. Accepted for publication July 9, 2020.

This work was supported by grants from the Deutsche Forschungsgemeinschaft to R.L. (SFB 796 TP B06 and SFB 1181 TP A06).

The microarray dataset presented in this article has been submitted to Gene Expression Omnibus (https://www.ncbi.nlm.nih.gov/geo/) under accession number GSE137150.

Address correspondence and reprint requests to Prof. Roland Lang, Institute of Clinical Microbiology, Immunology and Hygiene, University Hospital Erlangen, Wasserturmstrasse 3–5, D-91054 Erlangen, Germany. E-mail address: roland.lang@uk-erlangen.de

The online version of this article contains supplemental material.

Abbreviations used in this article: BMM, bone marrow–derived macrophage; cDMEM, complete DMEM; CLR, C-type lectin receptor; CT, threshold cycle; DC, dendritic cell; Gbp, GTPase-binding protein; GO, Gene Ontology; IRF1, IFN regulatory factor 1; KO, knockout; MHC-II, MHC class II; PAMP, pathogen-associated molecular pattern; qRT-PCR, quantitative real-time PCR; RT, room temperature; SOCS1, suppressor of cytokine signaling 1; SOCS1ΔNLS, nonnuclear SOCS1; SYK, spleen tyrosine kinase; TDB, trehalose-6,6-dibehenate; TDM, trehalose-6,6-dimycolate; TFBS, transcription factor binding site; WT, wild-type.

for inflammatory cytokine secretion (6), and strong Th1/Th17-promoting adjuvant activity to protein Ags (7)]. A synthetic analogue of the cord factor, trehalose-6,6'-dibehenate (TDB), together with a cationic liposome carrier, is an effective adjuvant in several experimental immunization models against intracellular pathogens (*M. tuberculosis* and *Chlamydia muridarum*) (8) and has been successfully tested in a phase I clinical trial in humans for generation of cellular immune responses to recombinant *M. tuberculosis* Ags (9).

Both TDM and TDB directly bind to the C-type lectin receptor (CLR) MINCLE (10, 11), encoded by the *Clec4e* gene in mouse and human (12, 13). The related CLR MCL is encoded by the *Clec4d* gene, located next to *Clec4e* on mouse chromosome 6, and has been identified as a second receptor for TDM (14). MCL and MINCLE can form heterodimers (15) and increase each other's protein level on the cell surface (16). MCL and MINCLE associate with the ITAM-containing adapter protein FcRγ (17), which is required for recruitment and activation of the spleen tyrosine kinase (SYK) in response to binding of TDM and TDB (18, 19). Downstream of SYK, PKCδ mediates phosphorylation of CARD9 (20), which, together with Bcl10 and Malt1, is required for IκB kinase activation and release of NF-κB from its inhibitor IκB (18). PI3 kinase signaling is also activated by TDM–MINCLE signaling and required for expression of several cytokines (21). The components of this pathway are essential to bring about inflammatory gene expression in response to TDM and TDB in vitro, as well as granuloma formation and adjuvanticity in vivo (10, 11, 18). These findings suggest that TDM and TDB induce very similar responses in macrophages because they both bind to and activate the MINCLE receptor; however, it has not been tested systematically at the genome-wide level whether there are also ligand-specific transcriptional responses.

Although a large body of evidence shows that the cord factor is a mycobacterial pathogen-associated molecular pattern (PAMP) activating innate immunity via MINCLE–SYK–CARD9 signaling, there is also evidence that TDM contributes to establishment of the *M. tuberculosis* intracellular niche. First, TDM delays phagosomal acidification and maturation (22). Second, stimulation of macrophages with mycobacteria depleted from cord factor by treatment with petroleum ether enhanced upregulation of co-stimulatory molecules and promoted killing of mycobacteria (23). Whether MINCLE signaling is also responsible for inhibitory effects of the cord factor on macrophages has not been studied in detail yet. Of interest, impaired phagosome acidification after FcγR-dependent phagocytosis of TDM-coated beads was indeed dependent on MINCLE and involved the phosphatase SHP-1 (24). Inhibitory effects of MINCLE ligation on murine dendritic cell (DC) activation and T cell priming capacity (25), and on induction of IL-12 in human DC and murine macrophages, have been reported recently (26, 27).

Inhibition of macrophage transcriptional responses to IFN-γ by *M. tuberculosis* has been investigated by the laboratories of Ernst and Boom. These studies demonstrated that IFN-γ signaling is not generally inhibited by *M. tuberculosis* because STAT1 phosphorylation of tyrosine 701 and serine 727, as well as nuclear translocation of STAT1, was intact (3). Killed mycobacteria and cell wall extracts were sufficient to inhibit IFN-γ–induced expression of FcγRI, leading to the identification of the mycobacterial TLR2 ligand 19-kDa lipoprotein as inhibitor of IFN-γ–induced CIITA and MHC-II expression (28, 29). Microarray-based profiling showed that *M. tuberculosis* infection and stimulation with the 19-kDa lipoprotein impaired the expression of a large subset of IFN-γ–induced genes (most notably of MHC-II genes) (28) but also synergized with IFN-γ to upregulate others (e.g., NOS2) (29). Thus, the current state of the literature shows that mycobacteria interfere with IFN-γ–induced upregulation of gene sets involved in Ag presentation at least in part through activation of TLR2 signaling in response to the 19-kDa lipoprotein. To what extent the cord factor, the most abundant glycolipid of the mycobacterial cell wall, contributes to a reprogramming of IFN-γ–induced gene expression has not been investigated yet.

In this study, we have performed a comprehensive transcriptome analysis of macrophages stimulated with TDB/TDM under resting or IFN-γ–cotreatment conditions. Both glycolipids caused largely overlapping transcriptional changes, consistent with triggering of the same receptor and pathway. TDB/TDM reprogrammed IFN-γ–induced gene expression by synergistically upregulating genes associated with the inflammatory response and by antagonizing a subset of IFN-γ target genes associated with Ag presentation via MHC-II and antimicrobial function such as selected members of the 65-kDa GTPase-binding protein (Gbp) family. Mechanistically, TDB/TDM blocked GBP1 expression at the level of transcription at least partially through MINCLE–FcRγ-dependent signaling. Although inhibition by TDB/TDM was independent of the negative regulators IL-10, NOS2, and type I IFN, we obtained evidence that it may involve IFN regulatory factor 1 (IRF1) activity. Suppressor of cytokine signaling 1 (SOCS1) was required for efficient inhibition of IFN-γ–induced gene expression, although TDM did not interfere with STAT1 phosphorylation. Together, our data reveal an ambiguous role of the cord factor in the cross-regulation of IFN-γ–signaling. It synergistically promotes IFN-γ–induced inflammatory chemokine and NOS2 expression in macrophages but, in contrast, antagonizes MHC-II Ag presentation and expression of selected antimicrobial GTPases. By this transcriptional reprogramming of IFN-γ responses, cord factor likely contributes to mycobacterial immune evasion and facilitates mycobacterial survival in the phagosome.

Materials and Methods

Reagents

TDB was obtained from Avanti Polar Lipids (Alabaster, AL), TDM was from Bioclot (Aidenbach, Germany). Murine rIFN-γ was purchased from PeproTech (Hamburg, Germany). Abs used for Western blot and immunofluorescence imaging are the following: for detection of GBP1, an mAb rat Ab (clone 2C4-1) provided by Dr. E. Naschberger (Erlangen, Germany) was used. Commercially available Abs were purchased for Grb2 (catalog no. 610112; BD), IRF1 (sc-640; Santa Cruz Biotechnology), STAT1 (sc-346; Santa Cruz Biotechnology), STAT1-pY701 (catalog no. 7649; Cell Signaling Technology).

Mice

C57BL/6, MINCLE–knockout (KO) (*Clec4e*$^{-/-}$), FcRγ-KO (*Fcerg1*$^{-/-}$), IRF1-KO (*Irf1*$^{-/-}$), and SOCS1-KO (*Socs1*$^{-/-}$; *Ifng*$^{-/-}$) were maintained under specific pathogen-free conditions in the animal facility of the Faculty of Medicine at the Friedrich-Alexander Universität Erlangen-Nürnberg (Präklinisches Experimentelles Tierzentrum). Bone marrow of MCL-KO (*Clec4d*$^{-/-}$) was kindly provided by Dr. B. Lepenies (Hannover, Germany). *Clec4d*$^{-/-}$ and *Clec4e*$^{-/-}$ mice have been described before and were generated by the Consortium for Functional Glycomics on a C57BL/6 background (19, 30). *Fcerg1*$^{-/-}$ were generated by Dr. Takai (31) and kindly provided by Dr. F. Nimmerjahn (Erlangen, Germany). Bones from *Socs1*$^{-/-}$*MGL*^{tg} mice (32) expressing nonnuclear SOCS1 (SOCS1ΔNLS) were prepared at the Department of Infectious Diseases at the University Hospital Heidelberg and shipped to Erlangen on wet ice.

Differentiation and stimulation of bone marrow–derived macrophages

Bone marrow–derived macrophages (BMM) were generated as described previously (33). In brief, bone marrow cells were isolated and, after erythrocyte lysis, cultured in complete DMEM (cDMEM) supplemented with 10% FCS, 1% penicillin/streptomycin (Sigma-Aldrich), 50 μM 2-ME, and 10% (v/v) M-CSF containing L cell–conditioned medium for 7 d.

After overnight depletion of adherent cells, 5–6 × 10^6 of the nonadherent cells were seeded per 10-cm petri dish. On day 3, 5 ml of cDMEM + 10% L cell–conditioned medium were added, and differentiated BMM were harvested on day 7 by treatment with Accutase for 10 min at 37˚C.

Glycolipids were dissolved in sterile isopropanol at a concentration of 2.5 mg/ml (TDB) and 1 mg/ml (TDM) and stored at −20˚C. Before coating of cell culture plates with glycolipids, the stock solutions were heated to 60˚C until the content was completely clear. Working solutions were then prepared in sterile isopropanol and distributed onto the culture wells as fast as possible. Isopropanol was evaporated in the laminar flow at room temperature (RT). The prepared culture plates were either used for stimulation directly or stored at 4˚C for a maximum of 1 wk. The final concentration in the cell culture well was 5 μg/ml for TDB and for TDM.

BMM were added at a density of 1 × 10^6 per milliliter in cDMEM. IFN-γ was used at a concentration of 50 ng/ml.

Cytokine detection by ELISA

Cytokines were quantified with sandwich ELISA sets from R&D Systems. The assay was performed in one quarter of the volumes given in the manual; otherwise, the procedure was performed according to manufacturer's instructions. Supernatants were routinely collected from 96-well plates after 48 h of stimulation and stored at −20˚C; for G-CSF ELISA, the supernatants were diluted 1:2 or 1:5 in 3% BSA in PBS. The OD was measured in an ELISA reader ($OD_{450\ nm}$–$OD_{650\ nm}$).

Griess assay for detection of nitrites

The Griess assay is an indirect method to quantify nitrogen oxide radical formation in cell culture. Supernatants of cell cultures were collected; first, 50 μl of supernatant were treated with 50 μl sulfanilic acid in phosphoric acid. The phosphoric acid removes the pH indicator phenol red, whereas the sulfanilic acid converts the NO^- radicals into nitrite (NO_2^-). The nitrite was then detected by adding 50 μl NED, which leads to formation of a pink color caused by an azo dye. The color formation was quantified by measuring the OD ($OD_{550\ nm}$–$OD_{650\ nm}$) in an ELISA plate reader and plotting it to a standard curve (2-fold dilution steps of sodium nitrite).

mRNA expression analysis

RNA isolation was performed by different methods. As a standard method, TriFast RNA isolation was used. In this study, 0.3 × 10^6 cells were cultured in 48-well plates and lysed in 0.3 ml TriFast (Peqlab Biotechnologie), or 0.5 × 10^6 were cultured in 24-well plates and lysed in 0.5 ml. The cleanup was performed according to manufacturer's instructions. Samples were washed twice with 0.1 ml 70% ethanol in diethyl pyrocarbonate–treated water. For large amounts of RNA samples, 0.2 × 10^6 cells were cultured in 96-well plates and lysed in 0.2 ml TriFast, and cleanup was performed with Zymo Direct-zol spin plates (Zymo Research Europe, Freiburg, Germany).

Where DNA digestion was required (genome-wide expression profiling, NanoString Elements and primary transcript quantitative real-time PCR [qRT-PCR]), RNA samples were isolated with Qiagen RNEasy Mini Kit (1 × 10^6 cells in 12-well plates) or Micro Kit (0.5 × 10^6 cells in 24-well plates). The procedure was performed according to the manufacturer's instructions (QIAGEN, Hilden, Germany). RNA samples were stored at −20˚C for short term and at −80˚C for long term.

For qRT-PCR, 0.5–1 μg total RNA was first reverse transcribed using random primers and the Applied Biosystems Prism High-Capacity cDNA Reverse Transcription Kit. cDNA samples were diluted to a final concentration of 5 ng/μl. qRT-PCR was used for relative quantitation by the ΔΔ threshold cycle (CT) method of mRNAs of interest, employing primer/probe combinations selected from the Universal Probe Library (https://lifescience.roche.com/en_de/brands/universal-probe-library.html#assay-design-center) and *Hprt* as a house-keeping gene. PCR reactions were performed in duplicates, and the mean CT values of target gene and of *Hprt* for technical replicates were used to calculate ΔCT values. Calibrator ΔCT values were calculated from biological replicates of control conditions (as indicated in the figure legends) and used to determine ΔΔCT values and fold-change values as $2^{-\Delta\Delta CT}$.

Genome-wide expression profiling

For genome-wide expression profiling, BMM from female C57BL/6 mice aged 6–8 wk were used for stimulation. Three completely independent experiments were performed. The BMM were stimulated in 12-well plates with 1 × 10^6 cells per well in 1 ml. TDB and TDM were coated to the culture wells; IFN-γ was added in solution. After 6 and 24 h, cells were harvested, and total RNA was prepared using Qiagen RNEasy Mini Kit, including DNAse treatment. Quality control on RNA samples was performed on an Agilent 2100 Bioanalyzer using the Eukaryote Total RNA Nano protocol according to manufacturer's instructions. Each sample had an RNA integrity number of 10 and a concentration of at least 50 ng/μl. Affymetrix Mouse Gene ST 2.0 was used as platform for the genome-wide expression profiling. Labeling, hybridization, and initial data analysis was performed by the Functional Genomics Core Unit at the Department of Human Genetics (University Hospital Erlangen). Quality control of the expression data was performed using Partek Genomic Suite. Intensity distribution was equal among the three replicates of the experiment. The data were then subjected to ANOVA, comparing two conditions of the same time point as well as comparing all conditions of the same time point. The resulting ANOVA tables were used to create gene lists as input for downstream analyses. The microarray dataset has been deposited in Gene Expression Omnibus with the accession number https://www.ncbi.nlm.nih.gov/geo/query/acc.cgi?acc=GSE137150.

Bioinformatic analyses of transcriptome data

The gene lists created in the ANOVA were subjected to Gene Ontology (GO) enrichment analysis in Cytoscape (version 3.2.1) using the plug-in Cluego (version 2.2.3). Standard threshold settings were used for the enrichment analysis (corrected p value <0.05; number of genes in cluster ≥ 3; percentage of genes in cluster ≥ 4; κ score 0.4). All enrichment analyses were performed using the whole genome as background. Ontologies used were biological process (database from March, 20, 2014), cellular component (November 6, 2015), and molecular function (November 6, 2015).

Western blot analyses

Whole-cell protein lysates were prepared from 1 × 10^6 cells stimulated in 12-well plates. After stimulation, cells were lysed in 0.1 ml radioimmunoprecipitation assay buffer with protease and phosphatase inhibitors on ice for 10 min. The lysates were sonicated in a Diagenode Bioruptor (5 min cycle on high with intervals 20 s on/20 s off) at 4˚C with a cooled water bath. Afterward, addition of 4× Lämmli buffer was supplemented with 2-ME, and the mixture was boiled (95˚C, 10 min) and then cooled on ice. Samples were loaded on an SDS-PAGE for protein separation, and Western blot was performed as wet blot onto a nitrocellulose membrane for 3 h at 300 mA with constant stirring. Afterwards, the membranes were blocked for 1 h in blocking buffer (3% BSA or 5% milk powder in TBST) and then incubated with the primary Ab overnight (4˚C). On the following day, the membranes were washed in TBST (3 × 10 min, RT), and the HRP-coupled secondary Ab was added (2 h, RT). The membranes were washed again in TBST (3 × 10 min, RT), and the chemiluminescent signals were detected using Immobilon Western HRP substrate in a ChemoCam Imager.

CFSE dilution assay

The CFSE dilution assay was used to quantify T cell proliferation triggered by activated macrophages. $CD4^+$ T cells were isolated from OT-II transgenic mice that express a TCR specific for OVA (34). BMM were generated from congenic Ly-5.1 mice (B6.SJL-*Ptprca Pepcb*/BoyJ) that express the surface marker CD45.1, allowing unambiguous distinction from the CD45.2 allele present in the OT-II mice used as T cell donors by flow cytometry. A total of 1 × 10^5 BMM per well were stimulated in 96-well F-plates with IFN-γ and/or TDB to characterize effects of the cord factor analogue on the capacity for Ag presentation. After 24-h incubation, the BMM were washed four times with RPMI 1640. Then, OVA peptide 323–339 (sequence ISQAVHAAHAEINEAGR), which binds to the C57BL/6 MHC-II molecule $I\text{-}A^b$ (35), was added to the cultures at a concentration of 1 μM together with the OT-II cells (1 × 10^5 per well).

$CD4^+$ T cells were isolated from spleen and mesenteric lymph nodes of OT-II transgenic mice. First, the tissues were passed through a 40-μm nylon mesh, and the resulting single-cell suspension was subjected to erythrocyte lysis (10 ml ammonium chloride for 10 min, RT); the lysis was stopped with MACS buffer (20 ml). The cells were now separated by surface markers via MACS: in a first step, APCs were labeled with anti-CD11b and anti-B220 beads and depleted by negative selection on an LD Column (all Miltenyi Biotec) according to the manufacturer's protocol. The remaining cells were positively selected for $CD4^+$ cells using CD4 beads and an LS Column (Miltenyi Biotec). A purity of >90% $CD4^+$ T cells was determined by flow cytometry, and the fraction was labeled with CFSE and added to the prepared APC cultures, together with OVA peptide. Proliferation of $CD4^+$ T cells was analyzed after 3 d by flow cytometry (FACSCanto II), gating on $CD45.2^+$ cells.

Immunofluorescence microscopy

Immunofluorescence microscopy was used to quantify nuclear levels of pSTAT1 and IRF1 upon IFN-γ (20 ng/ml) stimulation alone and in

combination with TDM (2 μg/ml). A total of 1.5×10^5 BMM were stimulated on coverslips (24-well plates) for 40 min (pSTAT1) or 4 h (IRF1), washed with PBS (two times), fixed with 2% paraformaldehyde in PBS (15 min RT), washed again (three times in PBS) and incubated with anti-CD11b APC (BioLegend) for 30 min for cell surface staining (1:200 dilution in 0.2% BSA in PBS, 4°C). Cells were washed again (three times in PBS) and permeabilized using frozen methanol (stored at −20°C, 2 min). Before quenching and blocking, cells were washed again (three times PBS) and incubated with goat serum diluted in quenching buffer (1:20 in NH_4Cl, 20 min, RT). Cells were then incubated with anti-pSTAT1 (Y701) (1:50; Cell Signaling Technology) or anti-IRF1 (1:50) Abs (20 min, RT), washed (three times in PBS), and stained with Alexa Fluor 488–conjugated anti-rabbit IgG secondary Ab (20 min, RT). Slides were mounted with Dianova mounting medium with DAPI. Samples were examined with a Zeiss LSM 700 and further analyzed with ZEN software. At least five images were taken from each slide (two biological replicates and three independent experiments), and in a further analysis signal, intensities of pSTAT1 and IRF1 of each cell nucleus were measured (brightness, arbitrary units). Overlapping cells were excluded from the analysis. The cumulative signal intensity of each nucleus was divided by the nucleus area and relative signal intensities of all cells recorded on one biological replicate were attributed to a class on a frequency matrix and divided by the total number of cells recorded. Next, the mean relative signal intensity of a brightness class from one condition was calculated (counts).

Statistical analysis

Data from expression profiling were preanalyzed and subjected to ANOVA in Partek Genomic Suite. No correction was performed because of small sample size.

Results

Divergent regulation of NOS2 and G-CSF expression in macrophages treated with IFN-γ and the MINCLE ligand TDM

We have previously shown that stimulation of macrophages with TDM and its synthetic analogue TDB induces expression of *NOS2* and of G-CSF in an MINCLE-dependent manner (11, 36). In this study, we were interested in the effects of combined stimulation with TDM and IFN-γ on macrophage activation. Expression of *NOS2* was moderately upregulated by the individual stimuli and displayed strong induction upon combination of TDM with IFN-γ (Fig. 1A). In contrast, G-CSF mRNA was strongly induced by TDM but much more weakly by IFN-γ, and the combination of TDM with IFN-γ did not further increase G-CSF expression but, in fact, decreased it at the higher IFN-γ concentration (Fig. 1B). These data suggested gene-specific interactions between MINCLE-dependent signaling triggered by TDM and the IFN-γR pathway.

Natural cord factor TDM and synthetic TDB induce highly similar transcriptome changes with little overlap to the IFN-γ–induced response

To assess the genome-wide effects of stimulation with the mycobacterial cord factor TDM and its synthetic analogue TDB on gene expression in resting and IFN-γ–treated macrophages, we performed comprehensive expression profiling using the Affymetrix Mouse Gene ST 2.0 platform using 6 and 24 h as early and late time points for analysis, respectively. To obtain robust datasets, the experiment was independently performed three times, allowing the application of stringent statistical and filtering criteria to identify significantly regulated genes. Comparison of TDB- and TDM-stimulated macrophages showed a somewhat stronger response after stimulation with natural cord factor than with synthetic glycolipid while demonstrating a large overlap (152/257 gene symbol-annotated transcripts after 6 h; 226/354 transcripts after 24 h) (Fig. 2A). In contrast, the set of IFN-γ–upregulated genes shared only a minor overlap with the TDB/TDM response (34/185 transcripts after 6 h; 27/163 transcripts after 24 h), consistent with

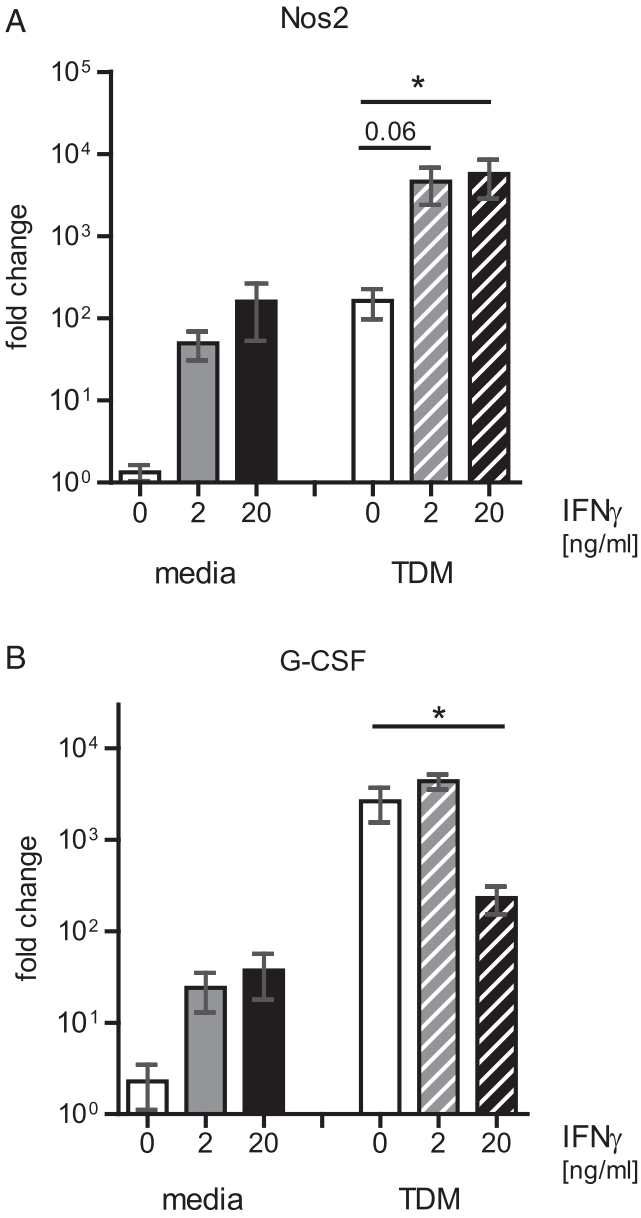

FIGURE 1. Differential regulation of NOS2 and G-CSF expression in macrophages treated with IFN-γ and the MINCLE ligand TDM. BMM were treated with plate-bound TDM (2 μg/ml) or IFN-γ (0, 2 or 20 ng/ml), alone or in combination. Expression of mRNA for G-CSF (**A**) and NOS2 (**B**) was analyzed 24 h after stimulation. Mean + SEM ($n = 10$ pooled from three independent experiments). Significant effects of IFN-γ on TDM-induced expression are indicated. *$p < 0.05$, unpaired t test.

the activation of distinct signaling pathways by IFN-γ versus the glycolipids.

GO analysis revealed that both TDB- and TDM-induced gene sets associated with inflammatory responses, leukocyte migration, and cytokine secretion and receptor binding (Fig. 2B). In contrast, the IFN-γ–induced gene set was enriched for GO terms associated with Ag presentation via MHC-I and MHC-II and for GTP-binding proteins (Fig. 2B). In silico analysis of promoters of gene sets induced by TDB or TDM showed shared enrichment of transcription factor binding sites (TFBS) for NF-κB family members, NFAT and its target gene *Egr1*, and of the MAPK-regulated transcription factors AP1 and CREB1 (Supplemental Fig. 1A), consistent with the established major signaling modules activated by CLR ligation (37, 38). The PU.1 family members SPIB and SPI1 are important

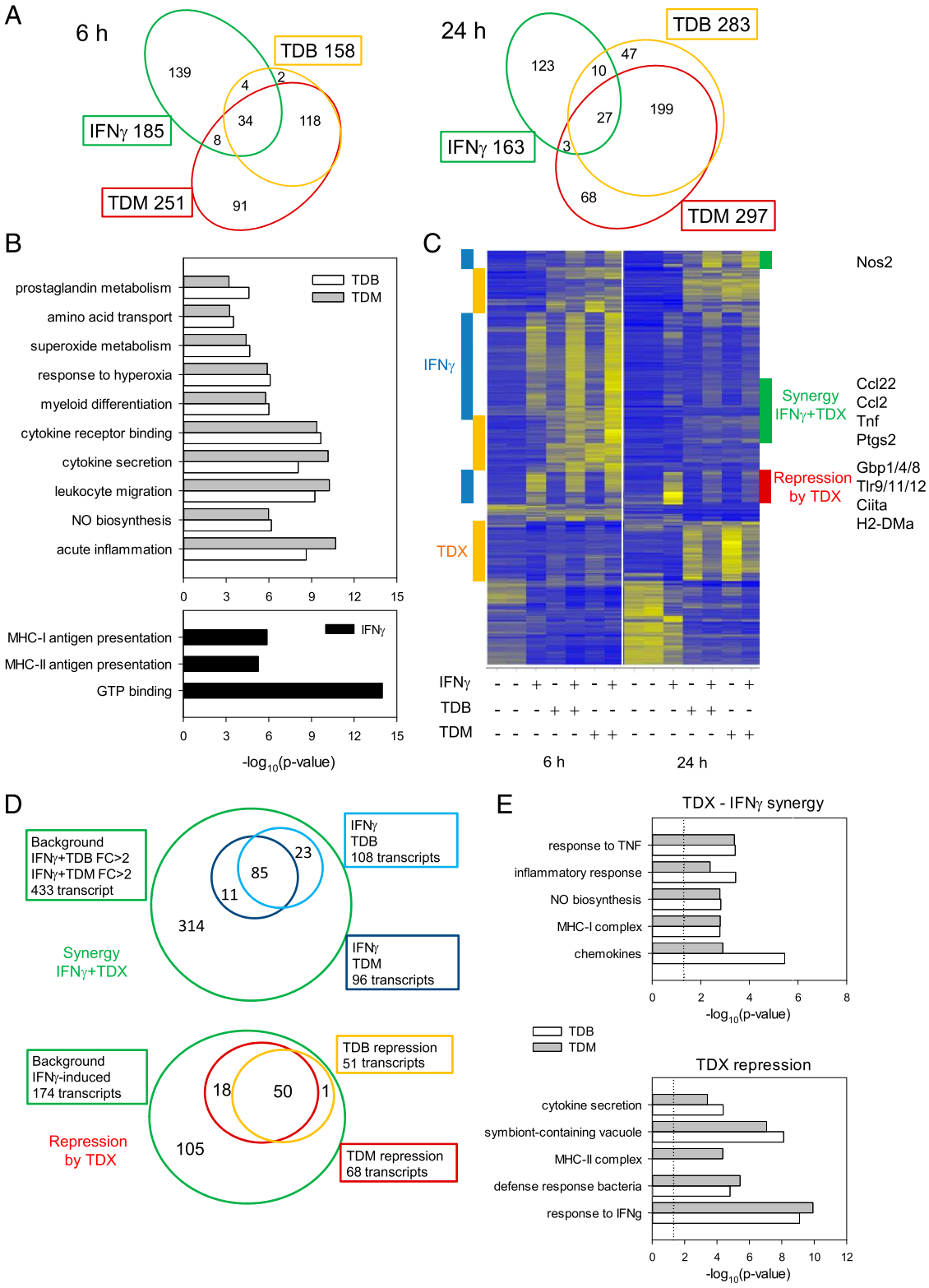

FIGURE 2. Genome-wide expression profiling of single or combined stimulation of macrophages with TDB/TDM and IFN-γ. BMM were treated for 6 and 24 h with TDB, TDM, and/or IFN-γ (50 ng/ml) as indicated. Total RNA from three independent experiments was labeled and hybridized to Affymetrix GeneChip Mouse Gene ST 2.0. Data analysis was done using Partek Genomic Suite to identify differentially regulated transcripts (ANOVA, $p < 0.05$; fold change (FC) versus mock control samples >2). (**A**) Venn diagrams showing the numbers of upregulated gene symbol-annotated transcripts after 6 h (left) and 24 h (right) after single stimulation with TDB, TDM, or IFN-γ. The sizes of common and unique sets of genes induced by the different stimuli are indicated. (**B**) GO terms enriched after stimulation with TDB/TDM or IFN-γ. The gene lists identified in (A) were analyzed using Cluego in all three ontologies (biological processes, cellular component, and molecular function). Only selected enriched terms are shown for clarity and to avoid redundant terms. Bars indicate $-\log_{10}$ (p value). (**C**) Heat map representation of 663 probesets (corresponding to 545 annotated genes) with >4-fold change in expression across all experimental conditions. Linearized average intensities were z-score normalized and subjected to hierarchical clustering (FlexArray 1.6.3., method: Complete). Yellow and blue coloring represents high and low expression, respectively. Gene clusters with TDB/TDM-induced expression are marked with blue bars and IFN-γ–induced ones in orange on the left side of the heat map. Gene groups with synergistic *(Figure legend continues)*

for macrophage differentiation and function and were enriched in the TDB/TDM-induced promoters at both time points. The early response genes were characterized by enrichment of CREB1, NFAT, EGR1, and IRF1, whereas the late response was enriched for TFBS less well characterized in macrophages (HOXA5, ZNF354C, and ARNT/AHR). The top-ranking enriched TFBS of the IFN-γ–induced genes were, as expected, IRF2 and IRF1, followed by NF-κB binding motifs and by STAT1 sites (Supplemental Fig. 1B).

Combined stimulation with TDM/TDB and IFN-γ reveals synergistic and antagonistic effects on gene expression programs

We next were interested in the effect of combined stimulation with glycolipids and IFN-γ on the macrophage transcriptome. We therefore selected a set of 663 transcripts (representing 545 annotated genes) (Supplemental Table I) that showed at least 4-fold regulation across all stimulation conditions and performed hierarchical clustering to obtain an overview of gene expression patterns (Fig. 2C). As expected (Fig. 2A), TDB and TDM (TDX) stimulation was highly similar but distinct from the response to IFN-γ. The combination of IFN-γ and the glycolipids led to several gene clusters showing overall higher signal compared with either stimulus alone (Fig. 2C), indicating synergistic effects at both time points. In contrast, a prominent cluster of IFN-γ–induced genes characterized by downregulation in the presence of TDX was apparent only at the 24-h time point, suggesting inhibitory effects of TDX on delayed induction of IFN-γ target genes (Fig. 2C). To quantitatively assess synergistic and repressive effects of TDX on the response to IFN-γ after 24 h, we next applied a combination of statistical significance and fold-change filtering criteria (Fig. 2D). Indeed, selecting the genes upregulated at least 2-fold by the combination of IFN-γ + TDX compared with nonstimulated macrophages, we found that a subset of ∼20% of genes was synergistically enhanced by combined versus single stimulation (Fig. 2D, upper panel), whereas an inhibitory effect of TDM/TDB stimulation on IFN-γ–induced gene expression was observed (50/174 genes downregulated by both TDM and TDB) (Fig. 2D, lower panel) (Supplemental Table II). Among the synergistically induced genes, several chemokines and inflammatory cytokines (e.g., CCL2, CCL22, and TNF) and inflammatory mediators (NOS2 and PTGS2) were found (Fig. 2C), consistent with the enrichment of the GO terms NO biosynthesis, chemokine activity, and inflammatory response (Fig. 2E). IFN-γ–induced genes subject to inhibition by TDM/TDB were enriched in the GO terms symbiont-containing vacuole, defense response to bacteria, and MHC-II complex, indicating interference of cord factor–induced signaling with the response to intracellular pathogens and with Ag presentation (Fig. 2E). Example genes for these terms were *Gbp1*, *Gbp4*, and *Gbp8* (defense response to bacteria) and *Ciita* and H2-DMa for MHC-II complex (Fig. 2C). In addition, TDM/TDB also impaired the IFN-γ–induced expression of several pattern recognition receptors (e.g., TLR9, TLR11, and TLR12).

TDB/TDM interfere with induction of MHC-II genes and Ag presentation by IFN-γ

A more detailed look at the regulation of MHC-II–related transcripts in the transcriptome dataset showed that indeed the IFN-γ–induced increase of expression for the classical MHC-II genes H2-Aa, H2-Ab1, and H2-Eb1 and the chaperone H2-DMa, as well as the master regulator of MHC-II expression, the transcription factor CIITA, were markedly impaired by concomitant stimulation with TDM or TDB (Fig. 3A). This inhibitory effect was confirmed in independent experiments using NanoString nCounter Elements and was partially dependent on the TDM receptor MINCLE (Fig. 3B). At the protein level, the low expression of the MHC-II molecule I-A^b on resting macrophages was as expected strongly enhanced by stimulation with IFN-γ after 24 and 48 h (Fig. 3C); cotreatment with TDB (Fig. 3C) or TDM (data not shown) moderately, but significantly, downregulated surface MHC-II protein levels after 48 h (Fig. 3C).

To determine whether the reduction of MHC-II expression by TDM/TDB exerts negative effects on the capacity of macrophages to elicit $CD4^+$ T cell responses to cognate Ag, we employed the OT-II TCR-transgenic mouse line with specificity for the OVA peptide ISQAVHAAHAEINEAGR ($OVA_{323–339}$) presented on MHC-II (34). Macrophages were incubated with $OVA_{323–339}$ and used as APCs for OT-II $CD4^+$ T cells labeled with CFSE (Fig. 3D). Pretreatment of macrophages with IFN-γ alone strongly increased T cell proliferation, but cotreatment of the macrophages with TDB and IFN-γ efficiently reduced the proliferative response of the OVA-specific T cells (Fig. 3D). Thus, although downregulation of the MHC-II protein IA^b on the macrophage surface by TDM/TDB was not very pronounced, the MHC-II–dependent activation of Ag-specific $CD4^+$ T cells was strongly suppressed by the glycolipids.

TDB/TDM impairs expression of several IFN-γ–induced 65-kDa GTPases through MINCLE-dependent signaling

The enrichment of GO terms associated with the response to infection with intracellular pathogens (host cell and symbiont-containing vacuole) in the set of IFN-γ–induced genes downregulated by TDM/TDB was due to several members of the family of 65-kDa IFN-γ–inducible GTPases, namely GBP1, GBP4, and GBP8. All 11 GBP family members were induced by IFN-γ in the transcriptome dataset, but only GBP1, GBP4, GBP8, and GBP11 showed significant downregulation when macrophages were costimulated with TDM/TDB (Fig. 4A). This pattern of regulation was confirmed in independent samples by NanoString nCounter analysis (Fig. 4B). Inhibition of mRNA expression for GBP1, GBP4, GBP8, and GBP11 by TDM was at least partially dependent on MINCLE signaling (Fig. 4B). GBP1 was the most strongly regulated family member in the extent of both the induction by IFN-γ as well as the inhibition by TDM/TDB. Of interest, GBP1 is recruited to the mycobacterial phagosome and is required for control of mycobacterial replication in macrophages in vitro and in mice in vivo (39). Therefore, we decided to investigate the inhibitory

upregulation by IFN-γ and TDX, and with repression of IFN-γ response by TDX, are indicated on the right side of the heat map in green and red, respectively. (**D**) Filtering for synergistic and antagonistic regulation of the IFN-γ response by TDX. For synergistically induced genes (upper panel), first, all transcripts with an FC >2 in the comparison of TDX + IFN-γ versus mock with a p values <0.05 were selected (Background); next, an FC filter >1.3 in the comparison TDX + IFN-γ versus IFN-γ and additional FC filters >1 in the comparisons IFN-γ versus mock and TDX versus mock were applied. For repression of IFN-γ–induced genes by TDX (bottom panel), we selected all transcripts with an FC >2 in the comparison IFN-γ versus mock as background; next, we applied an FC filter <1.5 for the comparison TDX + IFN-γ versus IFN-γ. (**E**) GO term enrichment of synergistically induced and TDX-repressed gene clusters. The gene lists identified in (D) were analyzed using Cluego in all three ontologies (biological processes, cellular component, and molecular function). Only selected enriched terms are shown for clarity. Bars indicate $-\log_{10}$ (p value). Dotted lines indicate a significant p value (0.05).

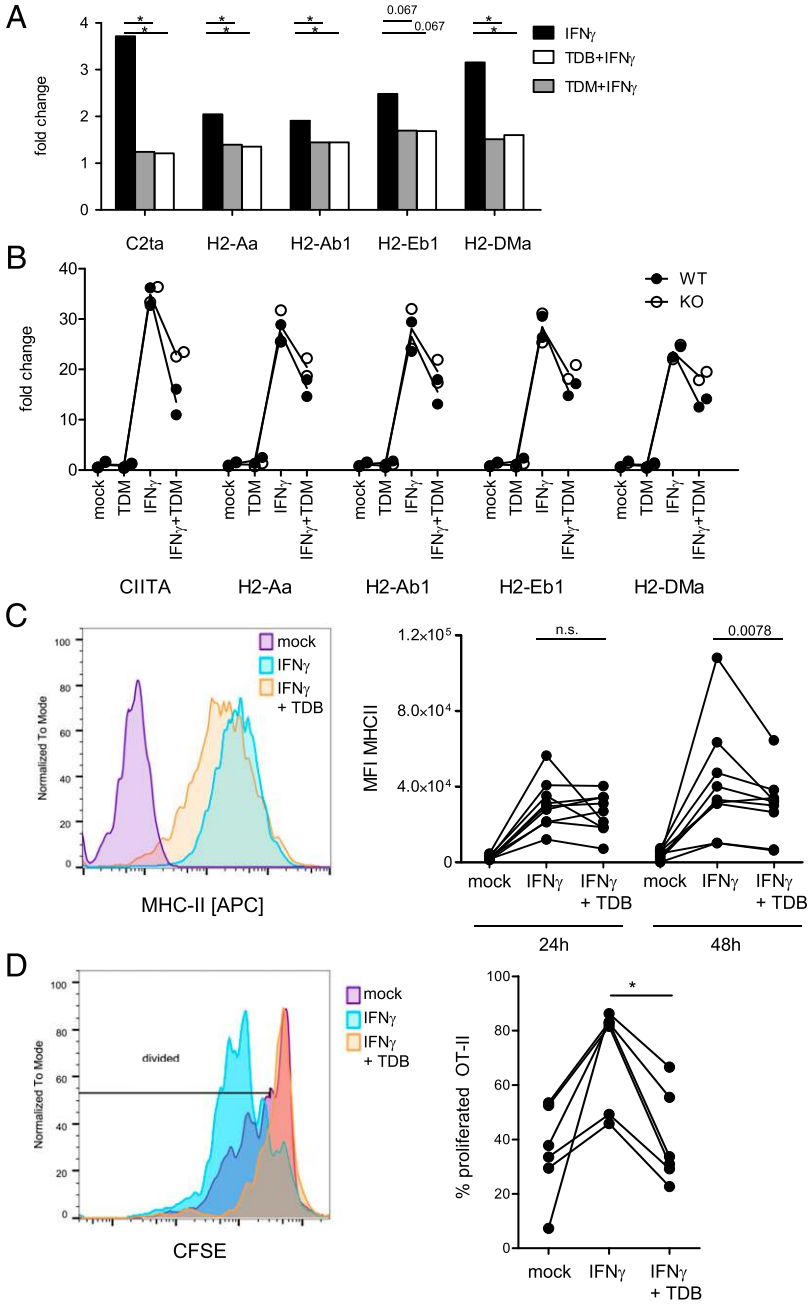

FIGURE 3. TDB/TDM interfere with induction of MHC-II genes and Ag presentation by IFN-γ. (**A**) Average signals of transcripts encoding classical MHC-II molecules and the master regulator Ciita from the Affymetrix transcriptome dataset were normalized to mock-treated controls to obtain fold-change values ($n = 3$). Time point: 24 h. Significant differences for the effect of TDX are indicated. *$p < 0.05$, Student t test. (**B**) Validation using NanoString technology with RNA samples from two additional independent experiments. Macrophages were stimulated as before with IFN-γ (50 ng/ml) and/or TDM for 24 h, followed by RNA preparation and processing for nCounter analysis. Signals were normalized to mock-treated WT samples to calculate fold-change values. Each dot represents RNA from one experiment. (**C**) Effect of TDB on cell surface MHC-II expression. BMM were stimulated in 96-well plates as indicated with IFN-γ (50 ng/ml) and/or plate-coated TDB for 24 or 48 h. MHC-II surface levels were stained with an APC-labeled Ab to I-A/I-E, with gating on live singlet cells (left panel). Right panel shows mean fluorescence intensity values for MHC-II from duplicate samples for six independent experiments; the p values in Wilcoxon signed-rank test are indicated for the effect of TDB on IFN-γ–treated BMM. (**D**) Reduced capacity of TDB-treated BMM to elicit Ag-specific proliferation of OT-II $CD4^+$ T cells. BMM from syngeneic $CD45.1^+$ mice on C57BL/6 background were stimulated (1×10^5 cells per well in 96-well F-plates) as indicated with IFN-γ and/or TDB for 24 h, followed by washing and addition of CFSE-labeled 1×10^5 OVA-specific $CD4^+$ T cells purified from the spleen of OT-II mice, together with cognate OVA peptide 323–339 (1 μM). Cells were harvested 72 h later and stained for CD45.2 (OT-II $CD4^+$ T cells), CD11b (BMM), and fixable viability dye for dead cell exclusion. Gating on live $CD45.2^+$ $CD4^+$ T cells, CFSE dilution as a measure of T cell proliferation was determined (overlay, left panel). The fraction of cells with ≥1 cell division from six independent experiments (averages of duplicate samples) is shown in the right panel. *$p < 0.05$, Wilcoxon signed-rank test.

action of the cord factor on GBP1 in more detail. Confirming the mRNA expression data on the protein level, we observed strong induction of GBP1 protein by Western blot and inhibition by the cord factor TDM in an MINCLE- and FcRγ-dependent manner (Fig. 4C, Supplemental Fig. 2). The related CLR MCL (encoded by *Clec4d*), a second receptor for TDM, was also required for TDM-induced blockade of GBP1 induction by IFN-γ (Supplemental Fig. 2).

TDM/TDB inhibit GBP1 expression at the level of transcription

In the microarray dataset, we observed prominent inhibition of IFN-γ–induced gene expression by TDM/TDB after 24 h but only minor inhibitory effects at the earlier 6-h time point. A kinetic analysis of IFN-γ– and TDM-regulated expression of several IFN-γ target genes revealed a continuing increase in GBP1 expression after IFN-γ stimulation over time until 48–72 h, whereas expression of Gbp2, Irf1, Cxcl10, and NOS2 peaked already between 4 and 24 h and declined afterward (Fig. 5A). The inhibition of GBP1 induction in macrophages treated in addition with TDM was not observed after 4 h but clearly visible after 24 h of stimulation and exceeded 90% thereafter (Fig. 5A). Similarly, GBP8 continued to increase in expression 24 h after stimulation with IFN-γ and was suppressed by TDM only starting at 24 h (Fig. 5A). To determine whether TDM interferes with the expression of GBP1 by destabilizing its mRNA, we blocked transcription by addition of actinomycin D to the macrophage cultures 24 h after stimulation with IFN-γ alone or the combination of TDM + IFN-γ and measured mRNA decay over time by qRT-PCR (Fig. 5B). Tnf was included in this analysis as prototypic unstable transcript and, indeed, was degraded with a half-life time of <30 min, independent of the presence of TDM (Fig. 5B, left panel). In contrast, GBP1 mRNA proved to be highly stable with no noticeable loss of mRNA until 8 h after addition of actinomycin D and no alteration by TDM (Fig. 5B, right panel). Primary transcript qRT-PCR for GBP1, using primers binding to intronic sequences, showed that the kinetics of induction of primary and mature GBP1 mRNA

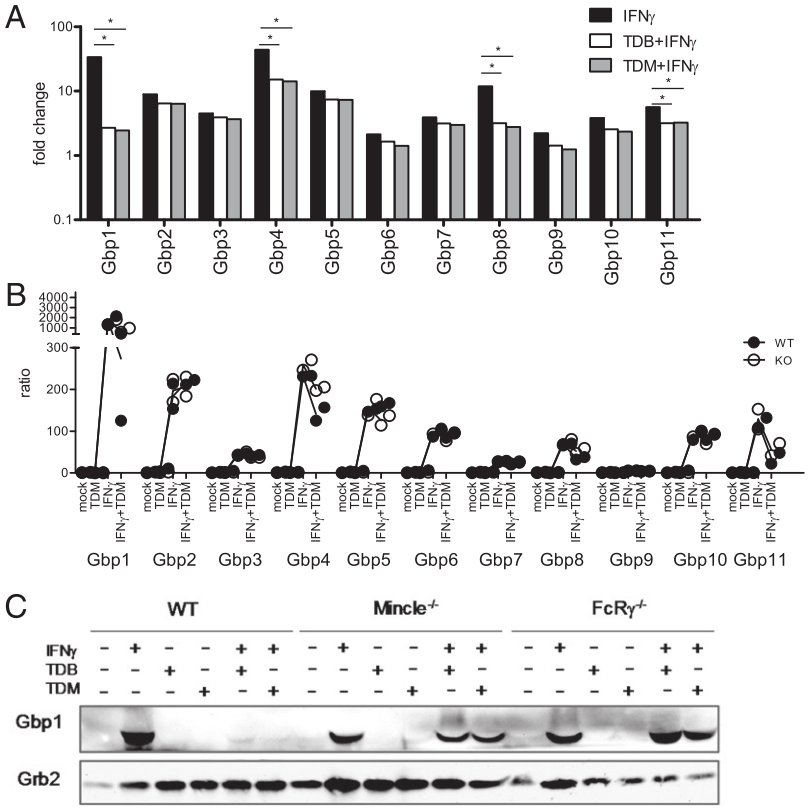

FIGURE 4. TDB/TDM impair expression of IFN-γ–induced 65-kDa GTPases GBP1, GBP4, GBP8, and GBP11. (**A**) Average signals of transcripts encoding GBP family members from the Affymetrix transcriptome dataset were normalized to mock-treated controls to obtain fold-change values ($n = 3$). Time point, 24 h. Significant differences for the effect of TDX are indicated. *$p < 0.05$, Student t test. (**B**) Validation using NanoString technology with RNA samples from two additional independent experiments. Macrophages were stimulated as before with IFN-γ (50 ng/ml) and/or TDM for 24 h, followed by RNA preparation and processing for nCounter analysis. Signals were normalized to mock-treated WT samples. Each dot represents RNA from one experiment. (**C**) TDB/TDM impair GBP1 protein expression after IFN-γ (50 ng/ml) stimulation dependent on MINCLE–FcRγ signaling. BMM were stimulated as indicated for 48 h. Total cell lysates were analyzed by Western blot for murine GBP1 and Grb2 as loading control. Representative for at least three experiments.

were comparable, and displayed a similar degree of inhibition by TDM, which was first observable after 3–5 h of stimulation and increased over time in both assays (Fig. 5C). Thus, both the induction of GBP1 expression by IFN-γ and the inhibition by costimulation with the cord factor occurred at the level of transcription, whereas mRNA stability was unaltered.

Intact initial response to IFN-γR stimulation in TDB/TDM-treated macrophages

The gene-specific nature of synergistic and antagonistic effects of costimulation with IFN-γ and TDM/TDB suggested that the initiation of signaling by IFN-γ is likely not inhibited by the cord factor. Based on the transcriptome data, the expression levels of the IFN-γR chain IFNGR1 was moderately reduced in macrophages cotreated with TDX and IFN-γ, whereas the IFNGR2 receptor subunit, the kinases JAK1 and JAK2, and the essential IFN-γR–associated transcription factor STAT1, as well as STAT2 and STAT3, were not downregulated by treatment with the cord factor (Fig. 6A). Activation of the latent transcription factor STAT1 by phosphorylation at tyrosine-701 occurred as expected with rapid kinetics and was not altered significantly by cotreatment with TDM even at the late phase (24–48 h) after IFN-γ stimulation when GBP1 protein could already be detected by Western blot (Fig. 6B). In addition, IRF1 protein was induced comparably over time in IFN-γ–stimulated cells independent of the presence of TDM (Fig. 6B). As both transcription factors need to be translocated to the nucleus to bind to IFN-γ–regulated promoters, we also assessed whether TDM stimulation may inhibit gene expression by diminishing nuclear levels of STAT1 or IRF1. However, as evident from immunofluorescence analysis shown in Fig. 6C, this was not the case. The important role of IRF1 in IFN-γ–induced GBP1 expression was confirmed using macrophages from *Irf1*$^{-/-}$ mice in which the inducibility by IFN-γ was more than 100-fold reduced (Fig. 6D). However, because IFN-γ upregulated GBP1 mRNA expression also in *Irf1*$^{-/-}$ macrophages still ~100-fold, we could employ them to test whether TDM does still inhibit GBP1 mRNA in the absence of IRF1. Interestingly, the inhibitory effect (around 80% in the control C57BL/6 macrophages) was largely abrogated in *Irf1*$^{-/-}$ macrophages (Fig. 6D). These data indicate that TDM may interfere with the *trans*-activating function of nuclear IRF1 in a gene-specific manner in the case of GBP1.

Gene-specific inhibition of IFN-γ responses by TDM is independent of IL-10, NOS2, and type I IFN signaling but requires Socs1

Because inhibition of IFN-γ–induced expression of GBP1 and of other target genes by TDM/TDB was only observed after 4–6 h and increased over time, it probably depended on the synthesis of new gene products downstream of TDM–MINCLE signaling. We therefore tested several established regulators of IFN-γ signaling for a potential role in inhibition of GBP1 expression by TDM/TDB. First, NO generated by the synergistically induced NOS2 is released robustly by macrophages in response to IFN-γ and TDM/TDB and can interfere with IFN-γ–signaling through nitrosylation of kinases and transcription factors (40). Second, the anti-inflammatory cytokine IL-10 is produced in response to TDM/TDB and can inhibit IFN-induced gene expression by interfering with STAT1 tyrosine phosphorylation (41). Third, the type I IFNs IFN-α and IFN-β are upregulated by CLR triggering (42) and can dampen IFN-γ responsiveness. Using KO macrophages for *NOS2* and the type I IFNR (*Ifnar1*$^{-/-}$) and a blocking Ab to the IL-10R, we did not find any effect on the induction of GBP1 by IFN-γ or on the inhibition by cotreatment with TDM (Supplemental Fig. 3A–C). Finally, we considered a role for SOCS1 that is induced by IFN-γ itself and inhibits JAK2 activity.

We employed BMM from *Socs1*$^{-/-}$ mice on an IFN-γ–deficient background, which circumvents the early lethality because of hyperinflammation caused by unrestrained IFN-γ signaling in the absence of Socs1 (43, 44). At saturating concentrations of IFN-γ

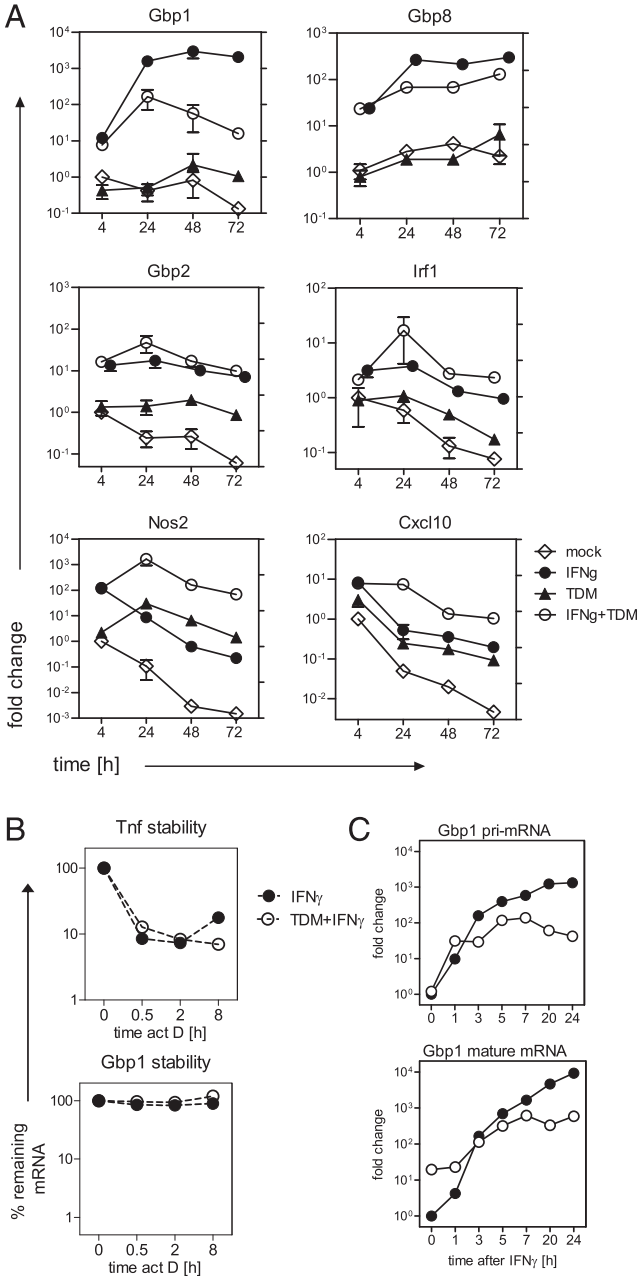

FIGURE 5. TDB/TDM inhibit GBP1 expression at the level of transcription. (**A**) Kinetics of GBP1 expression after stimulation with IFN-γ (50 ng/ml) and/or TDM. BMM were stimulated for the indicated time points, and mRNA levels were detected by qRT-PCR. Fold-change values were calibrated to mock-stimulated BMM at 4 h for all time points and conditions. Shown are mean and SD of biological duplicates from one representative experiment of at least two experiments with similar results. (**B**) GBP1 mRNA stability is high and not altered by TDM treatment. BMM were stimulated with IFN-γ or IFN-γ + TDM for 24 h, followed by addition of actinomycin D to stop transcription. RNA was harvested at the indicated time points and the relative amount of remaining transcripts for GBP1 and Tnf was determined by qRT-PCR. Average values of biological duplicates from one experiment. (**C**) Kinetic analysis of GBP1 primary transcript levels. BMM were pretreated with TDM or not overnight and then stimulated with IFN-γ at $t = 0$ h. Total RNA was prepared, DNAse treated, and reverse transcribed. Primary GBP1 transcript was amplified using intronic primers (upper panel); the mature, spliced GBP1 mRNA was detected with primers binding to exon 1 and exon 2 (lower panel). CT values were normalized to Hprt and calibrated to mock-treated samples at the 0-h time point. Data shown are averages of PCR duplicates from one representative of three experiments with similar results.

(50 ng/ml), TDM inhibited GBP1 expression by 90% in *Socs1*$^{+/+}$ macrophages but showed no inhibition in *Socs1*$^{-/-}$ macrophages (Fig. 7A). At lower concentrations of IFN-γ, the increased expression of GBP1 in *Socs1*$^{-/-}$ compared with *Socs1*$^{+/+}$ macrophages complicated the interpretation of the results, but still inhibition of GBP1 expression by TDM was much more pronounced in *Socs1*$^{+/+}$ than in *Socs1*$^{-/-}$ macrophages (Fig. 7A). Western blot for GBP1 protein levels confirmed the mRNA data, showing a nearly complete recovery of IFN-γ–induced GBP1 in TDM-treated *Socs1*$^{-/-}$ macrophages for the high concentration of IFN-γ (Fig. 7B). Thus, SOCS1 was required for the inhibitory effect of TDM–MINCLE signaling on expression of the IFN-γ target gene GBP1. The canonical function of SOCS1 is to downregulate IFN-γ signaling by binding to JAK2 and inhibiting its activity, thereby reducing IFN-γ–induced tyrosine 701 phosphorylation and activation of STAT1. However, STAT1 tyrosine 701 phosphorylation was not affected by cotreatment with TDM at the time points tested between 4 and 48 h (Fig. 6B). These results suggested that the function of SOCS1 in inhibition of GBP1 expression after stimulation with TDM may be independent of its canonical function as an inhibitor of IFN-γ–induced STAT1 activation. Recently, a nuclear function for SOCS1 in attenuating NF-κB activity through binding to p65 was revealed (45). To determine whether nuclear SOCS1 contributes to inhibition by TDM, we employed a BAC-transgenic mouse line expressing a mutant SOCS1 protein with a deletion of the nuclear localization sequence (SOCS1ΔNLS) (32). However, macrophages from the SOCS1ΔNLS mice, expressing SOCS1 exclusively in the cytoplasm, were equally efficient in inhibition of GBP1 expression by TDM as wild-type (WT) control macrophages (Fig. 7C). Together, the results indicate that cytoplasmic SOCS1 inhibits IFN-γ–induced GBP1 expression by a mechanism independent of JAK2 inhibition.

Discussion

The mycobacterial cord factor's Janus-faced properties as mycobacterial PAMP and potential virulence factor have fascinated infection immunologists for decades. Although the cord factor has strong proinflammatory and adjuvant properties, it also contributes to establishment of an intracellular niche in macrophages by delaying phagosomal maturation. In this study, we have used microarray-based transcriptome analysis to investigate the reprogramming of gene expression by the cord factor in resting and IFN-γ–activated murine macrophages. Our results reveal substantial synergistic and antagonistic effects of TDM/TDB and IFN-γ consistent with major functional effects of mycobacterial glycolipids on the macrophage response during infection. Synergistic gene expression was associated with leukocyte recruitment and proinflammatory cytokines, consistent with a role for cord factor recognition in granuloma formation and tissue inflammation. In contrast, TDM/TDB antagonized Ag presentation via MHC-II molecules and impaired the expression of antimicrobial IFN-γ–induced 65-kDa GTPases, which may functionally convert the macrophage into a mycobacteria-friendly environment. Consistent with gene-specific shaping of IFN-γ–induced transcriptional responses, cord factor did not significantly alter proximal signaling by the IFN-γR, such as phosphorylation and nuclear translocation of STAT1 or upregulation of the transcription factor IRF1. Inhibition of GBP1 expression by TDM required cytoplasmic SOCS1, which acts in a nonclassical mechanism independent of JAK2-STAT1 inhibition, whose molecular details remain to be elucidated.

Natural cord factor (TDM) and its synthetic analogue TDB both directly bind to the CLR MINCLE and require FcRγ–SYK–CARD9

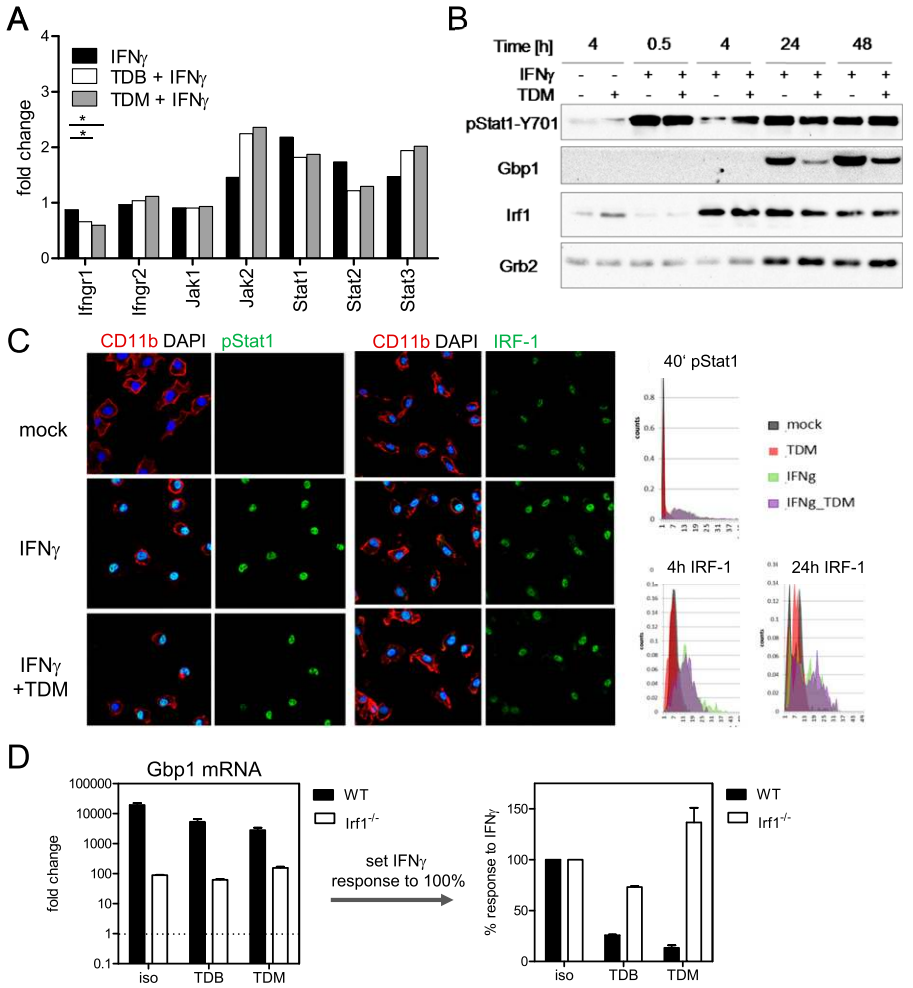

FIGURE 6. Intact initial response to IFN-γR stimulation in TDB/TDM-treated macrophages. (**A**) Expression levels IFN-γR–associated signaling proteins. Transcriptome data from the 24-h time point are depicted as mean fold-change values relative to mock-treated BMM ($n = 3$). *$p < 0.05$, by ANOVA for the decreased expression in the comparison of TDX + IFN-γ versus IFN-γ alone. (**B**) Phosphorylation of STAT1 on Tyr^{701} and expression of Irf1 is unaltered by treatment with TDM. WT BMM were stimulated with TDM and/or IFN-γ (50 ng/ml) for the indicated times. Total cell lysates were analyzed by immunoblot. Representative for at least three experiments with similar results. (**C**) Intact IFN-γ–induced nuclear translocation of STAT1 and IRF1. BMM stimulated as indicated were fixed, permeabilized, and stained with Abs to CD11b (red signal), pSTAT1 (left panel, green signal), or IRF1 (right panel, green signal). Nuclear staining was done with DAPI present in the mounting media. Immunofluorescence pictures were recorded on a Zeiss LSM 700 microscope. Shown are representative images of three independent experiments from 40 min after stimulation (pSTAT1) and 4 h after stimulation (IRF1). Original magnification ×200. For quantitative analysis, the signal intensity (brightness, arbitrary units [AU]) of each nucleus relative to its area was calculated. The relative brightness of all cells recorded from one biological replicate were attributed to classes of a frequency matrix and divided by the total number of cells recorded. Next, the mean relative signal intensity within one condition was calculated. The *y*-axis shows the relative frequency of a brightness class, and the *x*-axis shows the brightness (in classes of AUs). (**D**) GBP1 induction and inhibition in the absence of IRF1. WT and $Irf1^{-/-}$ BMM were stimulated with IFN-γ in the presence or absence of TDB/TDM for 24 h. GBP1 mRNA was measured by qRT-PCR and calibrated to WT mock controls (left panel). To quantitate the inhibitory effect of the glycolipids, fold-change values for IFN-γ only were set to 100% in both WT and $Irf1^{-/-}$ BMM, and the relative expression levels in the presence of TDB or TDM were calculated (right panel). Data are from one representative experiment of three performed (left panel) or mean and SEM from three (isopropanol; TDM) and two (TDB) experiments (right panel).

signaling to activate cytokine gene expression in macrophages. Our side-by-side comparison of TDM and TDB in the transcriptional profiling experiment showed largely overlapping sets of induced genes at both time points; in addition, GO term enrichment and TFBS analysis revealed no robust differences in the response to natural and synthetic glycolipid, which were both characterized by terms associated with inflammatory response, cytokine and chemokine production, leukocyte migration, and biosynthesis of PGs and NO. These results suggest that indeed both TDM and TDB signal primarily via MINCLE–FcRγ–SYK–CARD9 to activate macrophages. Of note, in an independent transcriptomic analysis, we recently observed a significant MINCLE-independent component of transcriptional regulation in response to TDM (21). In addition to MINCLE, the closely related CLR MCL is involved in the response to the cord factor (14, 16) and forms heterodimers with MINCLE (15). A CLR-independent pathway for transducing effects of TDM on macrophages was described through the scavenger receptor MARCO together with TLR2/4 activation (46) but was not further explored by us in this study.

To model the integration of signals received by macrophages during infection from mycobacteria and $CD4^+$ T cells recruited to the granuloma, we stimulated macrophages with IFN-γ and TDM, alone and concomitantly. Synergistic effects by combination of IFN-γ with TDX were observed for a subset of genes at both time points, pointing to cooperation of different activating transcription factors triggered by TDM–MINCLE signaling (e.g., NF-κB, NFAT, AP1, and CREB1) and the IFN-γR–activated pathway (STAT1 and IRF1). The set of synergistically induced genes was

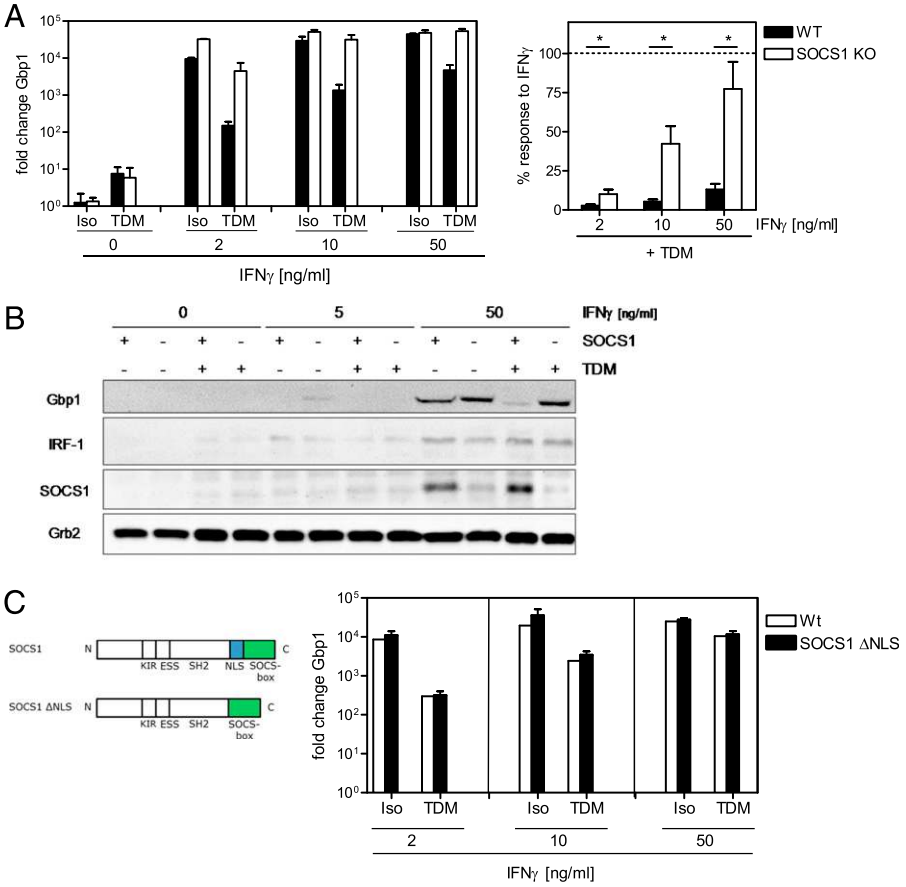

FIGURE 7. Socs1 is required for efficient inhibition of GBP1 expression by TDM. (**A**) Socs1$^{-/-}$ and Socs1$^{+/+}$ BMM on an IFN-γ$^{-/-}$ background were stimulated with titrated concentrations of IFN-γ in the presence or absence of TDM. GBP1 mRNA levels were measured after 24 h by qRT-PCR, normalized to Hprt, and calibrated to the nonstimulated Socs1$^{+/+}$ sample. Left panel, Mean and SD of two biological replicates from one representative experiment. Right panel, To quantitate the inhibitory effect of the glycolipids, fold-change values for each concentration of IFN-γ alone were set to 100% for the BMM from one mouse and the relative expression levels in the presence of TDM were calculated. Mean and SEM (n = 5 mice for both genotypes, pooled from three individual experiments). *$p < 0.05$. (**B**) Immunoblot analysis of Socs1$^{+/+}$ (+) and Socs1$^{-/-}$ (−) BMM stimulated for 24 h with IFN-γ and TDM as indicated. Similar results were obtained at least three independent experiments. (**C**) TDM inhibits IFN-γ–induced GBP1 expression in SOCS1ΔNLS BMM. Experimental conditions as in (A), using BMM carrying an SOCS1ΔNLS BAC transgene on an Socs1$^{-/-}$ background (n = 8 for both genotypes, pooled from three independent experiments). No significant differences between genotypes in Student t test.

enriched for inflammatory chemokines (CXCL9, CXCL10, and CXCL11), several nonclassical MHC-I genes (H2-Q6 and H2-G7), and the enzymes Ptgs2 (COX2) and NOS2. MINCLE increases NO production in synergy with a TLR2 ligand by increasing translation (47). Because NO inhibits NLRP3 activation and IL-1 (47), we determined whether NOS2 is required for inhibition of IFN-γR–induced response, which was not the case.

Inhibitory effects of TDM on IFN-γ–induced gene expression are likely to be relevant for mycobacterial immune evasion by antagonizing protective T cell–dependent macrophage functions. TDM impaired the upregulation of a significant subset of IFN-γ–induced genes, but only at the later 24-h time point, whereas after 6 h, no inhibition of IFN-γ response by TDM was observed, suggesting that TDM-induced inhibition was due to newly synthetized mediators. TDM impaired IFN-γ–induced genes that were associated with MHC-II Ag presentation (CIITA, H2-Ab1, and H2-DM) and host response to intracellular infection (GBP1, GBP4, and GBP8). These results pointed to a mechanism by which mycobacterial cord factor can interfere with essential protective host responses during infection and were therefore validated in detail.

The attenuation of IFN-γ–induced expression of MHC-II by the glycolipids observed in the microarray dataset was confirmed at the protein level, albeit the inhibitory effect of TDM/TDB was not very strong (Fig. 3C). However, the robust impairment of MHC-II–dependent CD4$^+$ T cell triggering by OVA peptide-pulsed, glycolipid-treated macrophages (Fig. 3D) suggests that cord factor–impeded Ag presentation is likely of functional relevance and may contribute to reduced CD4$^+$ T cell responses to *M. tuberculosis*–infected macrophages (48). Recent work indicates the functional importance of direct recognition of infected cells by CD4$^+$ T cells for control of tuberculosis (49). This inhibitory effect of TDM/TDB on Ag presentation by macrophages may seem paradoxical given the well-documented adjuvant activity of TDM (7) and its synthetic analogue TDB (8, 18, 50). However, during vaccination with TDM/TDB-containing adjuvants, T cell priming is likely mostly due to Ag presentation via DC in the draining lymph node. In contrast to macrophages, which constitutively express only low levels of MHC-II and depend on IFN-γ for robust upregulation (Fig. 3C), DC have high basal MHC-II surface protein levels that are actually not further enhanced by treatment with IFN-γ (51). Therefore, the inhibitory effect of TDM/TDB on MHC-II–dependent Ag presentation is likely only observed for macrophages but not for DC.

Inhibition of IFN-γ–induced MHC-II expression in macrophages by mycobacteria has been described previously (1, 28, 52, 53), and the TLR2 ligand 19-kDa lipopeptide was identified to prevent CIITA expression (28, 29, 54). Thus, our identification of a similar inhibitory effect for the major cell wall glycolipid shows that *M. tuberculosis* employs several PAMPs activating different pattern recognition receptor pathways to target IFN-γ–induced Ag presentation by macrophages. A synergistic inhibitory effect of TLR2 and MINCLE-dependent signaling on CIITA/MHC-II expression in mycobacteria-infected macrophages is therefore likely. We do not yet know by which mechanism TDM/TDB signaling interferes with CIITA/MHC-II expression. The laboratory of Boom and Harding (55) showed that the TLR2 ligand 19-kDa lipopeptide induced recruitment of C/EBPβ and C/EBPδ to the IFN-γ–inducible CIITA promoter, and that overexpression of the LIP isoform of C/EBPβ was sufficient to repress CIITA expression. Because C/EBPβ expression is upregulated by TDM–MINCLE signaling (19), a similar mechanism may be operating for cord factor–induced interference with IFN-γ–induced MHC-II expression. Inhibition of MHC-II–related gene expression by TDM was

only partially abolished in BMM lacking MINCLE; therefore, other pathways triggered by the cord factor are likely also involved. These may include other CLR such as MCL, the MARCO-TLR2/4, or currently unknown receptors.

The selective downregulation of IFN-γ–induced expression of the 65-kDa GTPases GBP1, GBP4, and GBP8 by TDM/TDB was of particular interest because of the established protective function of GBP1 in antimycobacterial defense (39). In fact, inhibition of GBP1 expression by mycobacteria was described previously (28). Again, it is likely that TLR- and CLR-dependent mycobacterial PAMPs work together to antagonize IFN-γ–dependent gene expression, in this case to evade the antimycobacterial effects of GBP1 at the phagosomal membrane (56). Repression of GBP1 by the cord factor required MINCLE–FcRγ signaling and was more pronounced at later time points, whereas the initial IFN-γ–induced increase in GBP1 expression measurable after 4–6 h was largely unaffected. Consistent with this kinetic pattern and the gene-specific nature of inhibition by the glycolipids, the initial signaling by the IFN-γR as detected by tyrosine phosphorylation and nuclear translocation of STAT1 was not impaired. Phosphorylation of STAT1 at Ser^{727} is another posttranslational modification required for its full transcriptional activity (57) that may be affected by TDM-induced signaling but was not tested by us yet. Upregulation and nuclear presence of the pivotal IFN-γ–induced transcription factor IRF1 was likewise not inhibited by cotreatment with TDM/TDB. In contrast, TDM–MINCLE negative regulation of GBP1 expression was abrogated in *Irf1*$^{-/-}$ macrophages, indicating that IRF1 activity may be targeted by TDM/TDB. In future work, it will be important to determine whether the gene-specific suppression of IFN-γ–induced gene expression correlates with reduced recruitment of STAT1 and IRF1 to the promoter/enhancer regions of genes like GBP1 or CIITA.

Because these data indicated the induction of a late-acting, gene-specific inhibitor of IFN-γ–induced transcriptional responses by TDM–MINCLE signaling, we tested several candidates. Although the negative regulators of macrophage activation IL-10, type I IFN, and NOS2 were not required for GBP1 suppression by TDM/TDB, we observed a significant reconstitution of GBP1 induction in Socs1-deficient macrophages at the mRNA and protein level. Socs1 is well established as inducible inhibitor of Jak2–STAT1 signaling (58), and its involvement in the downregulation of IFN-γ target genes expressed with delayed kinetics, such as GBP1, would be compatible with such a mode of action. However, we did not observe significant differences in STAT1 phosphorylation or nuclear accumulation in TDM-cotreated macrophages even at later time points, arguing against a canonical activity of Socs1 in this case. The use of SOCS1ΔNLS BAC-transgenic macrophages (32) allowed us to exclude that a nuclear function of Socs1, such as enhanced degradation of NF-κB p65 (45), is required for its inhibitory effect. Thus, the data suggest that TDM–MINCLE signaling employs a nonclassical cytoplasmic activity of SOCS1 to inhibit expression of late IFN-γ–induced genes, such as GBP1. The molecular details of how SOCS1 mediates TDM–MINCLE inhibitory functions remain to be elucidated but may involve targeting of specific signaling proteins in the IFN-γR pathway for degradation similar to its role in the downregulation of kinases and adapter proteins in the TLR pathway (59–61).In conclusion, using a reductionist experimental system, we explored the transcriptional reprogramming of macrophages by the mycobacterial cord factor and its analogue, the adjuvant TDB. Natural and synthetic glycolipid caused largely overlapping transcriptional upregulation, characterized by inflammatory cytokine and chemokine expression. TDM/TDB exerted ambiguous effects on macrophage transcriptional responses to the Th1 cytokine IFN-γ, with a strong synergistic effect on chemotactic and inflammatory mediators and antagonism of gene sets involved in Ag presentation via MHC-II and in antimicrobial host responses. The unbiased transcriptome data reveal two faces of cord factor in the macrophage–mycobacteria interaction: whereas sensing of mycobacterial TDM by the CLR MINCLE activates an innate inflammatory response required for leukocyte recruitment and granuloma formation, the same interaction impairs IFN-γ–induced Ag presentation and antimicrobial effector molecule expression. Thus, although recognition of TDM by MINCLE is likely beneficial for the host in the initial phase of infection, it may later enable the mycobacteria to persist long term in infected macrophages by interfering with host-protective signaling induced by T cell–derived IFN-γ.

Acknowledgments

We thank Manfred Kirsch for mouse husbandry and Katrin Jozefowski for technical assistance. We thank Dr. Bernd Lepenies (Hannover, Germany) for providing bone marrow of *Mcl*$^{-/-}$ mice.

Disclosures

The authors have no financial conflicts of interest.

References

1. Kincaid, E. Z., and J. D. Ernst. 2003. *Mycobacterium tuberculosis* exerts gene-selective inhibition of transcriptional responses to IFN-gamma without inhibiting STAT1 function. *J. Immunol.* 171: 2042–2049.
2. Noss, E. H., R. K. Pai, T. J. Sellati, J. D. Radolf, J. Belisle, D. T. Golenbock, W. H. Boom, and C. V. Harding. 2001. Toll-like receptor 2-dependent inhibition of macrophage class II MHC expression and antigen processing by 19-kDa lipoprotein of *Mycobacterium tuberculosis*. *J. Immunol.* 167: 910–918.
3. Ting, L. M., A. C. Kim, A. Cattamanchi, and J. D. Ernst. 1999. *Mycobacterium tuberculosis* inhibits IFN-gamma transcriptional responses without inhibiting activation of STAT1. *J. Immunol.* 163: 3898–3906.
4. Bekierkunst, A. 1968. Acute granulomatous response produced in mice by trehalose-6,6-dimycolate. *J. Bacteriol.* 96: 958–961.
5. Yarkoni, E., and H. J. Rapp. 1977. Granuloma formation in lungs of mice after intravenous administration of emulsified trehalose-6,6′-dimycolate (cord factor): reaction intensity depends on size distribution of the oil droplets. *Infect. Immun.* 18: 552–554.
6. Geisel, R. E., K. Sakamoto, D. G. Russell, and E. R. Rhoades. 2005. In vivo activity of released cell wall lipids of *Mycobacterium* bovis bacillus Calmette-Guérin is due principally to trehalose mycolates. *J. Immunol.* 174: 5007–5015.
7. Shenderov, K., D. L. Barber, K. D. Mayer-Barber, S. S. Gurcha, D. Jankovic, C. G. Feng, S. Oland, S. Hieny, P. Caspar, S. Yamasaki, et al. 2013. Cord factor and peptidoglycan recapitulate the Th17-promoting adjuvant activity of mycobacteria through mincle/CARD9 signaling and the inflammasome. *J. Immunol.* 190: 5722–5730.
8. Agger, E. M., I. Rosenkrands, J. Hansen, K. Brahimi, B. S. Vandahl, C. Aagaard, K. Werninghaus, C. Kirschning, R. Lang, D. Christensen, et al. 2008. Cationic liposomes formulated with synthetic mycobacterial cordfactor (CAF01): a versatile adjuvant for vaccines with different immunological requirements. *PLoS One* 3: e3116.
9. van Dissel, J. T., S. A. Joosten, S. T. Hoff, D. Soonawala, C. Prins, D. A. Hokey, D. M. O'Dee, A. Graves, B. Thierry-Carstensen, L. V. Andreasen, et al. 2014. A novel liposomal adjuvant system, CAF01, promotes long-lived *Mycobacterium tuberculosis*-specific T-cell responses in human. *Vaccine* 32: 7098–7107.
10. Ishikawa, E., T. Ishikawa, Y. S. Morita, K. Toyonaga, H. Yamada, O. Takeuchi, T. Kinoshita, S. Akira, Y. Yoshikai, and S. Yamasaki. 2009. Direct recognition of the mycobacterial glycolipid, trehalose dimycolate, by C-type lectin Mincle. *J. Exp. Med.* 206: 2879–2888.
11. Schoenen, H., B. Bodendorfer, K. Hitchens, S. Manzanero, K. Werninghaus, F. Nimmerjahn, E. M. Agger, S. Stenger, P. Andersen, J. Ruland, et al. 2010. Cutting edge: mincle is essential for recognition and adjuvanticity of the mycobacterial cord factor and its synthetic analog trehalose-dibehenate. *J. Immunol.* 184: 2756–2760.
12. Ostrop, J., K. Jozefowski, S. Zimmermann, K. Hofmann, E. Strasser, B. Lepenies, and R. Lang. 2015. Contribution of MINCLE-SYK signaling to activation of primary human APCs by mycobacterial cord factor and the novel adjuvant TDB. *J. Immunol.* 195: 2417–2428.
13. van der Peet, P. L., C. Gunawan, S. Torigoe, S. Yamasaki, and S. J. Williams. 2015. Corynomycolic acid-containing glycolipids signal through the pattern recognition receptor Mincle. *Chem. Commun. (Camb.)* 51: 5100–5103.
14. Miyake, Y., K. Toyonaga, D. Mori, S. Kakuta, Y. Hoshino, A. Oyamada, H. Yamada, K. Ono, M. Suyama, Y. Iwakura, et al. 2013. C-type lectin MCL is an FcRγ-coupled receptor that mediates the adjuvanticity of mycobacterial cord factor. *Immunity* 38: 1050–1062.

15. Lobato-Pascual, A., P. C. Saether, S. Fossum, E. Dissen, and M. R. Daws. 2013. Mincle, the receptor for mycobacterial cord factor, forms a functional receptor complex with MCL and FcεRI-γ. *Eur. J. Immunol.* 43: 3167–3174.
16. Miyake, Y., O. H. Masatsugu, and S. Yamasaki. 2015. C-type lectin receptor MCL facilitates Mincle expression and signaling through complex formation. *J. Immunol.* 194: 5366–5374.
17. Yamasaki, S., E. Ishikawa, M. Sakuma, H. Hara, K. Ogata, and T. Saito. 2008. Mincle is an ITAM-coupled activating receptor that senses damaged cells. *Nat. Immunol.* 9: 1179–1188.
18. Werninghaus, K., A. Babiak, O. Gross, C. Hölscher, H. Dietrich, E. M. Agger, J. Mages, A. Mocsai, H. Schoenen, K. Finger, et al. 2009. Adjuvanticity of a synthetic cord factor analogue for subunit *Mycobacterium tuberculosis* vaccination requires FcRgamma-Syk-Card9-dependent innate immune activation. *J. Exp. Med.* 206: 89–97.
19. Schoenen, H., A. Huber, N. Sonda, S. Zimmermann, J. Jantsch, B. Lepenies, V. Bronte, and R. Lang. 2014. Differential control of Mincle-dependent cord factor recognition and macrophage responses by the transcription factors C/EBPβ and HIF1α. *J. Immunol.* 193: 3664–3675.
20. Strasser, D., K. Neumann, H. Bergmann, M. J. Marakalala, R. Guler, A. Rojowska, K. P. Hopfner, F. Brombacher, H. Urlaub, G. Baier, et al. 2012. Syk kinase-coupled C-type lectin receptors engage protein kinase C-δ to elicit Card9 adaptor-mediated innate immunity. *Immunity* 36: 32–42.
21. Hansen, M., J. Peltier, B. Killy, B. Amin, B. Bodendorfer, A. Härtlova, S. Uebel, M. Bosmann, J. Hofmann, C. Büttner, et al. 2019. Macrophage phosphoproteome analysis reveals MINCLE-dependent and -independent mycobacterial cord factor signaling. *Mol. Cell. Proteomics* 18: 669–685.
22. Axelrod, S., H. Oschkinat, J. Enders, B. Schlegel, V. Brinkmann, S. H. Kaufmann, A. Haas, and U. E. Schaible. 2008. Delay of phagosome maturation by a mycobacterial lipid is reversed by nitric oxide. *Cell. Microbiol.* 10: 1530–1545.
23. Kan-Sutton, C., C. Jagannath, and R. L. Hunter, Jr. 2009. Trehalose 6,6′-dimycolate on the surface of *Mycobacterium tuberculosis* modulates surface marker expression for antigen presentation and costimulation in murine macrophages. *Microbes Infect.* 11: 40–48.
24. Patin, E. C., A. C. Geffken, S. Willcocks, C. Leschczyk, A. Haas, F. Nimmerjahn, R. Lang, T. H. Ward, and U. E. Schaible. 2017. Trehalose dimycolate interferes with FcγR-mediated phagosome maturation through Mincle, SHP-1 and FcγRIIB signalling. *PLoS One* 12: e0174973.
25. Iborra, S., M. Martínez-López, F. J. Cueto, R. Conde-Garrosa, C. Del Fresno, H. M. Izquierdo, C. L. Abram, D. Mori, Y. Campos-Martín, R. M. Reguera, et al. 2016. *Leishmania* uses Mincle to target an inhibitory ITAM signaling pathway in dendritic cells that dampens adaptive immunity to infection. *Immunity* 45: 788–801.
26. Wevers, B. A., T. M. Kaptein, E. M. Zijlstra-Willems, B. Theelen, T. Boekhout, T. B. H. Geijtenbeek, and S. I. Gringhuis. 2014. Fungal engagement of the C-type lectin mincle suppresses dectin-1-induced antifungal immunity. *Cell Host Microbe* 15: 494–505.
27. Patin, E. C., S. Willcocks, S. Orr, T. H. Ward, R. Lang, and U. E. Schaible. 2016. Mincle-mediated anti-inflammatory IL-10 response counter-regulates IL-12 in vitro. *Innate Immun.* 22: 181–185.
28. Pai, R. K., M. E. Pennini, A. A. Tobian, D. H. Canaday, W. H. Boom, and C. V. Harding. 2004. Prolonged toll-like receptor signaling by *Mycobacterium tuberculosis* and its 19-kilodalton lipoprotein inhibits gamma interferon-induced regulation of selected genes in macrophages. *Infect. Immun.* 72: 6603–6614.
29. Pennini, M. E., R. K. Pai, D. C. Schultz, W. H. Boom, and C. V. Harding. 2006. *Mycobacterium tuberculosis* 19-kDa lipoprotein inhibits IFN-gamma-induced chromatin remodeling of MHC2TA by TLR2 and MAPK signaling. *J. Immunol.* 176: 4323–4330.
30. Wells, C. A., J. A. Salvage-Jones, X. Li, K. Hitchens, S. Butcher, R. Z. Murray, A. G. Beckhouse, Y. L. Lo, S. Manzanero, C. Cobbold, et al. 2008. The macrophage-inducible C-type lectin, mincle, is an essential component of the innate immune response to *Candida albicans*. *J. Immunol.* 180: 7404–7413.
31. Kaifu, T., J. Nakahara, M. Inui, K. Mishima, T. Momiyama, M. Kaji, A. Sugahara, H. Koito, A. Ujike-Asai, A. Nakamura, et al. 2003. Osteopetrosis and thalamic hypomyelinosis with synaptic degeneration in DAP12-deficient mice. *J. Clin. Invest.* 111: 323–332.
32. Zimmer, J., M. Weitnauer, S. Boutin, G. Küblbeck, S. Thiele, P. Walker, F. Lasitschka, L. Lunding, Z. Orinska, C. Vock, et al. 2016. Nuclear localization of suppressor of cytokine signaling-1 regulates local immunity in the lung. *Front. Immunol.* 7: 514.
33. Lang, R., R. L. Rutschman, D. R. Greaves, and P. J. Murray. 2002. Autocrine deactivation of macrophages in transgenic mice constitutively overexpressing IL-10 under control of the human CD68 promoter. *J. Immunol.* 168: 3402–3411.
34. Robertson, J. M., P. E. Jensen, and B. D. Evavold. 2000. DO11.10 and OT-II T cells recognize a C-terminal ovalbumin 323-339 epitope. *J. Immunol.* 164: 4706–4712.
35. Barnden, M. J., J. Allison, W. R. Heath, and F. R. Carbone. 1998. Defective TCR expression in transgenic mice constructed using cDNA-based alpha- and beta-chain genes under the control of heterologous regulatory elements. *Immunol. Cell Biol.* 76: 34–40.
36. Huber, A., R. S. Kallerup, K. S. Korsholm, H. Franzyk, B. Lepenies, D. Christensen, C. Foged, and R. Lang. 2016. Trehalose diester glycolipids are superior to the monoesters in binding to Mincle, activation of macrophages in vitro and adjuvant activity in vivo. *Innate Immun.* 22: 405–418.
37. Geijtenbeek, T. B., and S. I. Gringhuis. 2016. C-type lectin receptors in the control of T helper cell differentiation. *Nat. Rev. Immunol.* 16: 433–448.
38. Ostrop, J., and R. Lang. 2017. Contact, collaboration, and conflict: signal integration of Syk-coupled C-type lectin receptors. *J. Immunol.* 198: 1403–1414.
39. Kim, B. H., A. R. Shenoy, P. Kumar, R. Das, S. Tiwari, and J. D. MacMicking. 2011. A family of IFN-γ-inducible 65-kD GTPases protects against bacterial infection. *Science* 332: 717–721.
40. Bogdan, C. 2015. Nitric oxide synthase in innate and adaptive immunity: an update. *Trends Immunol.* 36: 161–178.
41. Ito, S., P. Ansari, M. Sakatsume, H. Dickensheets, N. Vazquez, R. P. Donnelly, A. C. Larner, and D. S. Finbloom. 1999. Interleukin-10 inhibits expression of both interferon alpha- and interferon gamma- induced genes by suppressing tyrosine phosphorylation of STAT1. *Blood* 93: 1456–1463.
42. del Fresno, C., D. Soulat, S. Roth, K. Blazek, I. Udalova, D. Sancho, J. Ruland, and C. Ardavín. 2013. Interferon-β production via dectin-1-Syk-IRF5 signaling in dendritic cells is crucial for immunity to C. albicans. *Immunity* 38: 1176–1186.
43. Marine, J. C., D. J. Topham, C. McKay, D. Wang, E. Parganas, D. Stravopodis, A. Yoshimura, and J. N. Ihle. 1999. SOCS1 deficiency causes a lymphocyte-dependent perinatal lethality. *Cell* 98: 609–616.
44. Alexander, W. S., R. Starr, J. E. Fenner, C. L. Scott, E. Handman, N. S. Sprigg, J. E. Corbin, A. L. Cornish, R. Darwiche, C. M. Owczarek, et al. 1999. SOCS1 is a critical inhibitor of interferon gamma signaling and prevents the potentially fatal neonatal actions of this cytokine. *Cell* 98: 597–608.
45. Strebovsky, J., P. Walker, R. Lang, and A. H. Dalpke. 2011. Suppressor of cytokine signaling 1 (SOCS1) limits NFkappaB signaling by decreasing p65 stability within the cell nucleus. *FASEB J.* 25: 863–874.
46. Bowdish, D. M. E., K. Sakamoto, M. J. Kim, M. Kroos, S. Mukhopadhyay, C. A. Leifer, K. Tryggvason, S. Gordon, and D. G. Russell. 2009. MARCO, TLR2, and CD14 are required for macrophage cytokine responses to mycobacterial trehalose dimycolate and *Mycobacterium tuberculosis*. *PLoS Pathog.* 5: e1000474.
47. Lee, W. B., J. S. Kang, W. Y. Choi, Q. Zhang, C. H. Kim, U. Y. Choi, J. Kim-Ha, and Y. J. Kim. 2016. Mincle-mediated translational regulation is required for strong nitric oxide production and inflammation resolution. *Nat. Commun.* 7: 11322.
48. Harding, C. V., and W. H. Boom. 2010. Regulation of antigen presentation by *Mycobacterium tuberculosis*: a role for toll-like receptors. *Nat. Rev. Microbiol.* 8: 296–307.
49. Srivastava, S., and J. D. Ernst. 2013. Cutting edge: direct recognition of infected cells by CD4 T cells is required for control of intracellular *Mycobacterium tuberculosis* in vivo. *J. Immunol.* 191: 1016–1020.
50. Desel, C., K. Werninghaus, M. Ritter, K. Jozefowski, J. Wenzel, N. Russkamp, U. Schleicher, D. Christensen, S. Wirtz, C. Kirschning, et al. 2013. The Mincle-activating adjuvant TDB induces MyD88-dependent Th1 and Th17 responses through IL-1R signaling. *PLoS One* 8: e53531.
51. Muhlethaler-Mottet, A., L. A. Otten, V. Steimle, and B. Mach. 1997. Expression of MHC class II molecules in different cellular and functional compartments is controlled by differential usage of multiple promoters of the transactivator CIITA. *EMBO J.* 16: 2851–2860.
52. Fulton, S. A., S. M. Reba, R. K. Pai, M. Pennini, M. Torres, C. V. Harding, and W. H. Boom. 2004. Inhibition of major histocompatibility complex II expression and antigen processing in murine alveolar macrophages by *Mycobacterium* bovis BCG and the 19-kilodalton mycobacterial lipoprotein. *Infect. Immun.* 72: 2101–2110.
53. Kincaid, E. Z., A. J. Wolf, L. Desvignes, S. Mahapatra, D. C. Crick, P. J. Brennan, M. S. Pavelka, Jr., and J. D. Ernst. 2007. Codominance of TLR2-dependent and TLR2-independent modulation of MHC class II in *Mycobacterium tuberculosis* infection in vivo. *J. Immunol.* 179: 3187–3195.
54. Pai, R. K., M. Convery, T. A. Hamilton, W. H. Boom, and C. V. Harding. 2003. Inhibition of IFN-gamma-induced class II transactivator expression by a 19-kDa lipoprotein from *Mycobacterium tuberculosis*: a potential mechanism for immune evasion. *J. Immunol.* 171: 175–184.
55. Pennini, M. E., Y. Liu, J. Yang, C. M. Croniger, W. H. Boom, and C. V. Harding. 2007. CCAAT/enhancer-binding protein beta and delta binding to CIITA promoters is associated with the inhibition of CIITA expression in response to *Mycobacterium tuberculosis* 19-kDa lipoprotein. *J. Immunol.* 179: 6910–6918.
56. Kim, B. H., J. D. Chee, C. J. Bradfield, E. S. Park, P. Kumar, and J. D. MacMicking. 2016. Interferon-induced guanylate-binding proteins in inflammasome activation and host defense. *Nat. Immunol.* 17: 481–489.
57. Varinou, L., K. Ramsauer, M. Karaghiosoff, T. Kolbe, K. Pfeffer, M. Müller, and T. Decker. 2003. Phosphorylation of the Stat1 transactivation domain is required for full-fledged IFN-gamma-dependent innate immunity. *Immunity* 19: 793–802.
58. Starr, R., and D. J. Hilton. 2003. Defining control: regulation of dendritic cell activation and immune homeostasis by SOCS1. *Immunity* 19: 308–309.
59. Eberle, M. E., and A. H. Dalpke. 2012. Dectin-1 stimulation induces suppressor of cytokine signaling 1, thereby modulating TLR signaling and T cell responses. *J. Immunol.* 188: 5644–5654.
60. Mansell, A., R. Smith, S. L. Doyle, P. Gray, J. E. Fenner, P. J. Crack, S. E. Nicholson, D. J. Hilton, L. A. J. O'Neill, and P. J. Hertzog. 2006. Suppressor of cytokine signaling 1 negatively regulates toll-like receptor signaling by mediating Mal degradation. *Nat. Immunol.* 7: 148–155.
61. Trinath, J., S. Holla, K. Mahadik, P. Prakhar, V. Singh, and K. N. Balaji. 2014. The WNT signaling pathway contributes to dectin-1-dependent inhibition of toll-like receptor-induced inflammatory signature. *Mol. Cell. Biol.* 34: 4301–4314.